ACS OMEGA

Open Access

http://pubs.acs.org/journal/acsodf

Article

Molecular Imprints of Clinical Comorbidities in Hypothalamic Extracellular Vesicles at the Onset of Obesity

María Fernández-Rhodes,[¶] Manuel Suárez,[¶] Itziar Molet, Susana Suárez-García, Lluís Arola, Siu Kwan Sze, Xavier Gallart-Palau,* and Aida Serra*

Cite This: *ACS Omega* 2025, 10, 23563−23581

Read Online

ACCESS | Metrics & More | Article Recommendations | Supporting Information

ABSTRACT: The onset of obesity is characterized by early physiological and molecular changes, including leptin resistance and hypothalamic dysfunction, preceding significant weight gain and metabolic complications. Extracellular vesicles (EVs) are key mediators of intercellular communication, reflecting early pathological shifts in metabolic disorders. This study investigates the role of hypothalamic EVs (hEVs) in early obesogenic insult and their potential implications for obesity-related comorbidities. Using a hamster model fed a high fat diet for 30 days, next-generation proteomics revealed altered hEV protein compositions linked to cellular metabolism, neuroinflammation, and metabolic dysfunction, mirroring early obesity-related dysfunction. These findings highlight the adaptive molecular profiles of hEVs during early obesogenic insult and their potential as biomarkers and molecular mediators in obesity progression and its comorbidities. In conclusion, this study provides new insights into the molecular mechanisms underlying the onset of obesity and highlights hEVs as promising targets for early detection and intervention.

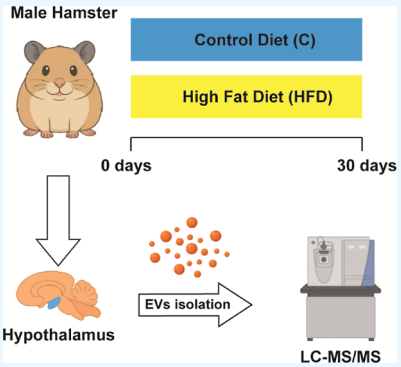

INTRODUCTION

Obesity is a multifactorial condition characterized by excessive energy intake, leading to the accumulation and growth of adipose tissue. According to the World Obesity Atlas 2023, the global prevalence of obesity is currently estimated at 38%, reflecting a significant health crisis worldwide.[1] The increase in obesity rates has been observed across various regions, driven by the joint influence of unhealthy food selections and a more sedentary way of living. This trend has affected populations in both high-income and low- to middle-income countries, with notable rises in Southeast Asia and the Western Pacific regions.[2,3] Furthermore, projections indicate that by 2030, global obesity will affect 1.12 billion individuals, with an additional 2.16 billion people categorized as overweight, representing approximately 51% of the global population.[4] This alarming trend is expected to impose a massive economic burden on health systems worldwide. The rapid increase in obesity prevalence underscores the urgent need for comprehensive and effective public health interventions to combat this growing epidemic across diverse populations.

The onset of obesity is characterized by early physiological changes, such as the development of leptin resistance and hypothalamic dysfunction, which impair the regulation of energy balance.[5] Leptin, a hormone secreted by adipocytes, is a key regulator of appetite and energy expenditure through its actions on hypothalamic pathways. In the early stages of obesity, peripheral hyperleptinemia occurs as a compensatory response to increased adiposity; however, leptin receptor signaling in the hypothalamus becomes impaired, leading to the development of leptin resistance.[6] This disruption marks a critical window in the progression of obesity, where molecular and physiological alterations are initiated before significant weight gain or long-term metabolic dysfunction manifests.[7]

Extracellular vesicles (EVs) are nanosized particles delimited by a lipid bilayer which are secreted and commonly taken up by all cell types within the central nervous system (CNS).[8] These vesicles carry proteins, lipids and microRNA (miRNAs), among other relevant molecules.[9−11] Over the last decades, the role of these vesicles has been widely explored from being considered "cellular dust" to collaborating in the evolution of cancer and other pathologies. One of the main roles of EVs is their participation in intra- and interorgan communication, due to their capacity to reflect the state of their parental cells.[12] For instance, EVs are participating in the communication of adipose tissue with other peripheral organs, such as skeletal muscle or liver.[13−15] On the other hand, EV-like particles have been associated with the CNS development and activity. EVs are widely active in Neural progenitor cells (NPCs), which are activated in adult hypothalamus, regulate neurogenesis, gliogenesis[16,17] and neuroinflammation.[18,19] In addition, it has been established that autocrine communication mediated

Received: March 11, 2025
Revised: May 9, 2025
Accepted: May 16, 2025
Published: May 29, 2025

https://doi.org/10.1021/acsomega.5c02274
ACS Omega 2025, 10, 23563−23581

by EVs allows for the exchange of molecular information across the blood−brain barrier (BBB), as demonstrated by several studies.[20−22] Our extensive prior research in the field, as well as that of our colleagues, has also shown that analyzing CNS-EVs through next-generation proteomics and advanced Systems Biology offers highly valuable insights into the molecular mechanisms involved in neuropathology as well as brain and endocrine disorders.[23−28] Understanding how hEVs adapt their molecular cargo during the onset of obesity could provide crucial insights into the mechanisms underlying the early stages of this condition and its associated comorbidities.

In this study, we investigate the molecular makeup of hypothalamic EVs (hEVs) in a well-established high fat diet (HFD) Syrian hamster model. Our goal is to determine whether these specific vesicles alter their compositions at the onset of obesity, to better understand the underlying molecular mechanisms that may contribute to, and potentially provide novel biological markers for, obesity-related comorbidities.

MATERIALS AND METHODS

Reagents and Chemicals. All reagents were purchased from Sigma-Aldrich (St. Louis, MO, USA) unless otherwise specified. Protease inhibitor cocktail tables were obtained from Roche (Basel, Switzerland). Sequencing-grade trypsin was purchased from Promega (Madison, WI, USA).

Animal Studies. All animals were housed individually at 22 °C under a 12 h light/dark cycle and had free access to food and water. Ten-week-old hamsters (Charles River Laboratories, Barcelona, Spain) weighing 110−120 g were divided in two groups (n = 8 in each group). The control group stayed in a normal-fat diet (NFD) for 30 days and the other group was maintained in an isocaloric HFD for 30 days. The NFD has 11% of its calories from fat, while the HFD consists of 23% calories from fat and includes 1 g/kg of cholesterol. The sample size was calculated with the statistical program G*Power (version 3.1.9.4). Food intake and body weight were recorded weekly, with food being renewed daily. At the end of the study, all experimental animals were sacrificed under anesthesia (pentobarbital sodium, 60 mg/kg body weight) after a 6 h daytime fast and brains were excised. The hypothalamic region was dissected and stored at −80 °C until analysis. The animal protocol was approved by the Animal Ethics Committee of the Technological Unit of Nutrition and Health of Eurecat (Reus, Spain) and the Generalitat de Catalunya (DAAM 10026), and all of procedures were performed in accordance to the European Communities Council Directive (86/609/EEC). The experimental protocol was conducted in accordance with the EU Directive 2010/63/EU for animal experiments and adhered to the ARRIVE guidelines and the "Principles of Laboratory Animal Care".

Plasmatic Leptin Determination. Leptin concentrations in plasma samples from hamsters were quantified using a commercially available enzyme-linked immunosorbent assay (ELISA) kit (ELK Biotechnology, Denver, USA). The assay was performed according to the manufacturer's instructions. Standards were prepared in parallel to generate a calibration curve. Absorbance readings were obtained using a microplate reader BioTek Epoch 2 Reader (Agilent, Santa Clara, USA) at 450 nm, and leptin concentrations were calculated based on the standard curve. All samples were analyzed in triplicate to ensure the accuracy and reproducibility of the measurements.

Isolation of Hypothalamic Extracellular Vesicles. Brain EVs were obtained by PROSPR-brain, as previously described.[29] Briefly, hypothalamic brain tissues from each animal (∼100 mg in weight) were carefully dissected and homogenized using detergent-free homogenization buffer consisting of 100 mM ammonium acetate supplemented with protease inhibitor cocktail tablets, with the aim of preserving EV fractions.[29,30] This process was carried out using the tissue homogenizer bullet blender (Next Advance, NY, USA). Metallic beads from Next Advance, with diameters ranging from 0.9 to 2.0 mm, were washed in triplicate with 1× PBS for 30 min before being mixed with brain tissues at a 1:1 ratio (w/w). All procedures were conducted at 4 °C. The brain homogenization process consisted of four cycles, with each cycle involving the addition of 300 μL of homogenization buffer and 5 min of homogenization. The first two cycles were conducted at medium intensity, while the last two cycles were performed at maximum intensity. Following each cycle, the homogenate was centrifuged at 15,000g for 10 min, and the resulting supernatants were combined. Detergent-free homogenates were mixed with four volumes of chilled acetone (−20 °C), vortexed, and then centrifuged at 5000g for less than 1 min. The resulting supernatants containing hydrophobic EV fractions were concentrated to near dryness using a vacuum concentrator (Concentrator Plus, Eppendorf AG, Hamburg, Germany).

Bicinchoninic Acid Assay. Bicinchoninic acid assay solution (B9643-1L, Supelco, Merck, USA) and copper(II) sulfate solution (C2284-25 ML, Sigma-Aldrich, Merck, USA) were used, according to the manufacturer's instructions to estimate EV protein concentrations. 25 μL of each sample was loaded in a 96-well plate, followed by 200 μL of BCA/copper complex solution. The absorbance was measured at 562 nm in a BioTek microplate reader.

Morphometric Characterization of Hypothalamic Extracellular Vesicles. Representative fractions of hEVs were characterized using NTA, following established protocols.[27,31,32] NTA was performed with a Nanosight NS300 sCMOS instrument (Malvern, UK) under the following conditions: a capture time of 60 s, camera level set to 4, slider shutter at 50, slider gain at 100, frames per second (FPS) at 32.5, syringe pump speed at 100, and a sample volume of 1 mL. The viscosity range was maintained between 0.906 and 0.910 cP, with the temperature set at approximately 24 °C. The analyses did not restrict any specific areas, allowing for the random screening of freely flowing samples.

Ultrastructural Characterization of Hypothalamic Extracellular Vesicles. Representative hEV samples were prepared for TEM analysis. hEV samples were applied onto Cu-Formvar-carbon grids and allowed to settle for 20 min at room temperature. The grids were then washed with HPLC water, and hEV preparations were fixed with 1% glutaraldehyde in PBS for 5 min. Following fixation, hEVs were stained with uranyl oxalate for 5 min and embedded in methyl-cellulose-uranyl-oxalate before being air-dried for permanent preservation. Electron micrographs were taken using a Jeol Jem 1010 electron microscope operated at 80 kV. The ultrastructural images were scale-calibrated, bileveled, and analyzed with the open-source software ImageJ (National Institutes of Health, Bethesda, MD, USA).

In-Solution Tryptic Digestion of Hypothalamic Extracellular Vesicles. hEVs underwent vesicle lysis and protein denaturation under 16 M urea prepared in 100 mM ammonium bicarbonate (ABB) as previously described.[25] Following a 20 min incubation at room temperature, the

https://doi.org/10.1021/acsomega.5c02274
ACS Omega 2025, 10, 23563−23581

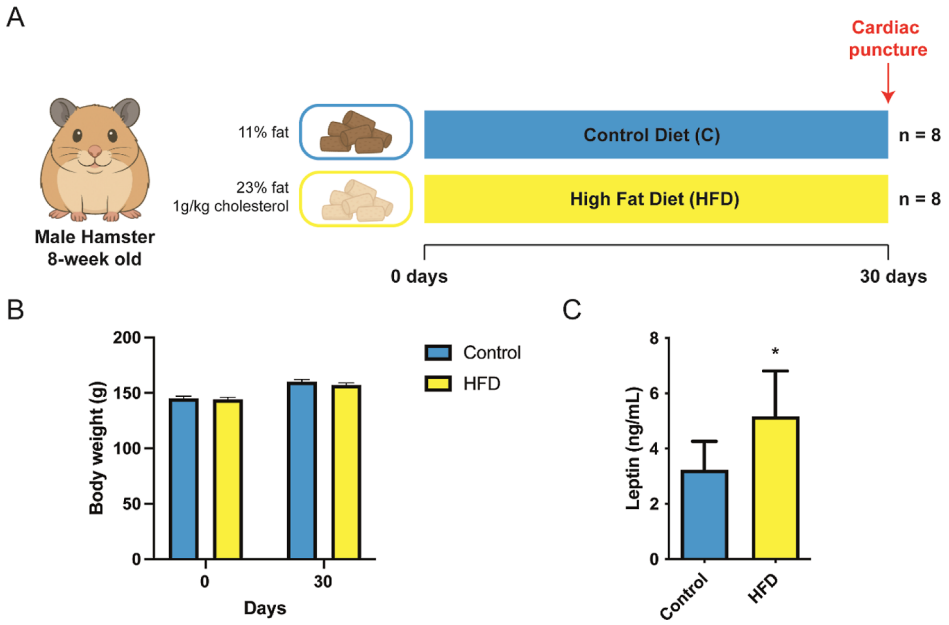

Figure 1. Experimental overview of the study and validation of the leptin-resistance model in Syrian gold hamster. (A) Illustrative diagram depicting the experimental design used in this study. (B) Animal body weight comparison between control animals (controls) and high fat diet (HFD)-treated animals at the beginning of the study (day 0) and at the end of the study (day 30). (C) Leptin quantification assessed by ELISA at the end of the study (30 days). Significant differences were assessed by student *t*-test. *indicates significant differences at $p \leq 0.05$.

samples were diluted with HPLC-grade water to achieve a final concentration of 8 M urea in 50 mM ABB. hEVs proteomes were reduced with 20 mM dithiothreitol at 30 °C for 3 h and alkylated with 40 mM iodoacetamide for 1 h at room temperature, protected from light. Subsequently, trypsin digestion was carried out overnight at 37 °C by adding 20 μg of sequencing-grade trypsin, followed by quenching with a final concentration of 0.5% formic acid (FA). The tryptic digested hEVs peptidome was desalted using a 100 mg C18 Sep-pack cartridge (Waters, Milford, MA). Elution of peptides was performed using 1 mL of 75% acetonitrile, 0.1% FA. The eluates were then dried using a vacuum concentrator and stored at −20 °C until further proteomics analysis.

High Pressure Liquid Chromatography Fractionation of Samples. Tryptic digested proteomes were fractionated with slight modifications to previously described methods.[29,30,33] Separation was conducted using a PolyWAX chromatographic column (4.6 × 200 mm, 3 μm, PolyLC, Columbia, MD, USA) on a Shimadzu Prominence UFLC system, monitored at 280 nm. Tryptic digested peptides were separated over a 72 min gradient at a flow rate of 1 mL/min. Mobile phase A consisted of 90% acetonitrile (ACN) and 0.1% acetic acid, while mobile phase B consisted of 10% ACN and 0.1% FA. The gradient was programmed as follows: 0% mobile phase B for 5 min, 0%−20% mobile phase B for 25 min, 20%−33% mobile phase B for 10 min, 33%−60% mobile phase B for 10 min, 60%−100% mobile phase B for 5 min, and 100% mobile phase B for 17 min. Fractions were collected every minute and combined into approximately 12 pooled fractions based on peak intensities. The combined fractions were then dried using a vacuum concentrator and reconstituted in 3% ACN and 0.1% FA for analysis by liquid chromatography-coupled tandem mass spectrometry (LC−MS/MS).

Liquid Chromatography Tandem-Mass Spectrometry Analysis of Hypothalamic Extracellular Vesicles Proteomes. Reconstituted pooled fractions (~2 μg proteins/fraction) were analyzed by LC−MS/MS using a Dionex UltiMate 3000 UHPLC system coupled to an Orbitrap Elite mass spectrometer (Thermo Fisher Inc., Bremen, Germany). A Michrom Thermo CaptiveSpray nanoelectrospray ion source, operating at a voltage of 1.5 kV, was used for sample spraying. Peptides were separated on a reverse-phase Acclaim PepMap RSL column (75 μm ID × 15 cm, 2 μm particle size from Thermo Fisher Inc.) maintained at 35 °C with a flow rate of 300 nL/min. The 60 min gradient used for separation of peptides was as follows: 3% mobile phase B (90% ACN, 0.1% FA) and 97% mobile phase A (0.1% FA in water) for 1 min, followed by 3%−35% mobile phase B over 47 min, 35%−50% mobile phase B over 4 min, 50%−80% mobile phase B over 6 s, maintained isocratically at 80% mobile phase B for 78 s. The gradient was then reverted to initial conditions over 6 s and maintained isocratically for 6.5 min. Data acquisition was performed in positive mode using Thermo Xcalibur 2.2 SP1.48 software (Thermo Fisher Inc.), alternating between full Fourier Transform mass spectrometry (FT-MS) (350−1600 m/z, resolution 60,000 at 400 m/z, with one μscan per spectrum) and Fourier transform tandem mass spectrometry (FT-MS/MS) (automatic mass range detection with a fixed first mass of 100 m/z, resolution 15,000 at 400 m/z, one μscan per spectrum). The 10 most intense ions were fragmented using high-energy collisional dissociation mode with 32% normalized collision energy. Automatic gain control values of 1×10^6 for FT-MS and 1×10^5 for FT-MS/MS were used.

Data Analysis and Bioinformatics. The proteomics raw data obtained from EVs was analyzed using an in-house Mascot server (version 2.6.02, Matrix Science, MA), with a precursor ion tolerance of 30 ppm and a fragment ion tolerance of 0.02 Da. The *Mus musculus* Uniprot database was used for searching the proteomics data (downloaded on 19th February of 2016, 101382 sequences and 43.874.034 residues). Deamidation at N and Q and oxidation of M were set as variable modifications, while cabarmydomethyl of C was set as

https://doi.org/10.1021/acsomega.5c02274
ACS Omega 2025, 10, 23563−23581

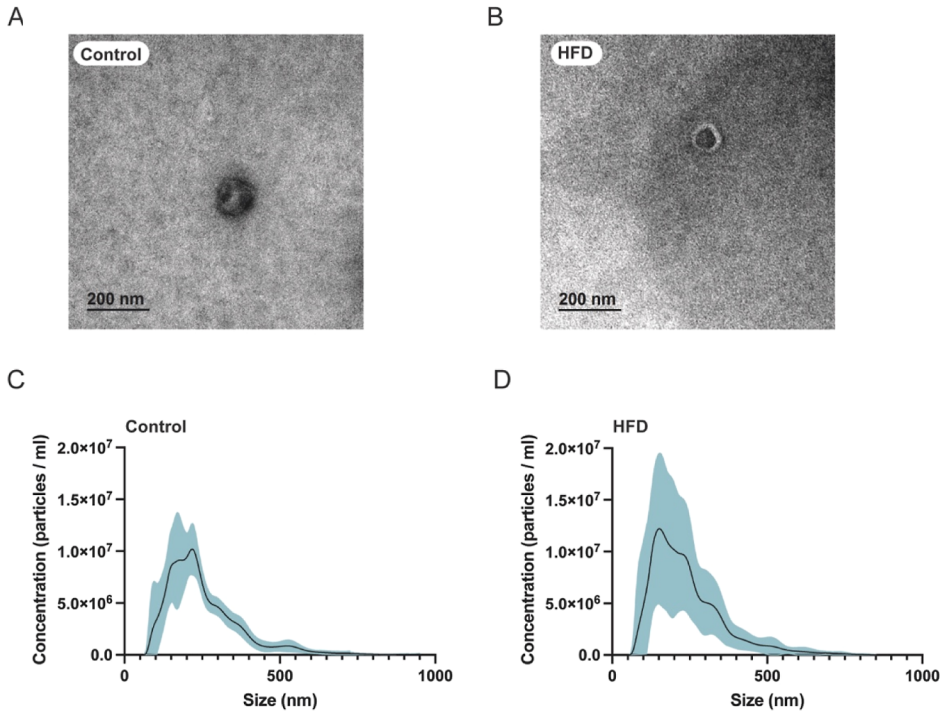

Figure 2. Ultrastructural and molecular characterization of hypothalamic extracellular vesicles (hEVs). Representative micrographs of hEVs obtained by electron transfer microscopy (TEM) from (A) control animals and (B) high fat diet (HFD)-treated animals. Average distribution profiles obtained by nanoparticle tracking analysis of hEVs from (C) control animals and (D) HFD-treated animals.

fixed modification. FDR < 1% was established for protein identification, and trypsin was set as proteolytic enzyme. Obtained data was exported to Microsoft Excel CSV files, and in-house generated macros were utilized for protein quantification analyses. Label-free quantitation of protein abundance was conducted using the exponentially modified protein abundance index (emPAI) in Mascot.[34] Only proteins present in three or more biological replicates in a group and absent in four or more biological replicates in the other were considered. Pathway analysis was conducted using the Mass Profiler Professional software version 15.1 from Agilent with the Wikipathways database. Protein−protein interaction analysis was conducted using the Search Tool for the Retrieval of Interacting Genes/Proteins STRING (v12.0; https://string-db.org). Significant differences were assessed by student *t*-test and statistical significance was set at $p \leq 0.05$, unless otherwise specified.

RESULTS

The Molecular Onset of Obesity in HFD. In this study, Syrian golden hamsters were subjected to a dietary intervention to investigate the molecular imprint of obesity during its onset in hypothalamic extracellular vesicles (hEVs). Over 30 days, animals were fed a high fat diet (HFD) rich in cholesterol, while the control group received a standard control diet. An overview of the experimental design is included in Figure 1A. Despite no significant differences in body weight between the HFD and control groups after the HFD intervention (Figure 1B), the HFD-fed hamsters showed a marked increase in plasma leptin levels compared to controls (Figure 1C). These findings demonstrates early metabolic disruption and leptin signaling alteration induced by the HFD-early obesogenic insult, validating the model as a reliable system to study diet-related metabolic dysregulation at the onset of obesity.

Physicochemical Properties of hEVs in HFD. After 30 days of HFD treatment, hEVs were isolated to investigate their structural, physical, and proteomic characteristics. These analyses aimed to identify the molecular signatures associated with early obesity-related metabolic disruptions in the hypothalamus. Ultrastructural and physical characterization of hEVs performed by transmission electron microscopy (TEM) and Nanoparticle Tracking Analysis (NTA), respectively, indicated that hEVs showed a rounded and membrane delimited structure with a mean diameter size of 182.0 ± 45.58 nm, without significant differences between experimental groups (Figure 2A−D).

The particle size distribution ranged from 57.40 to 690.9 nm, with 10% of particles showing an average diameter of 129.8 nm and 90% showing a mean diameter of 231.5 nm. (Figure 2A−D). The observed size distribution of hEVs indicates a significant presence of exosome- and microvesicle-like particles.

Proteomic characterization of hEVs revealed significantly higher number of proteins identified in hEVs from HFD-treated animals compared to controls (Figure 3A, Data sets S1 and S2). Despite these differences, no significant changes were observed in total protein abundance between the groups (Figure 3A). Further analysis compared the hEV proteomes with data from the specialized Vesiclepedia database, providing detailed insights into the presence and abundance of specific EV markers in these preparations (Figure 3B). This analysis identified 100 EV markers exclusively present in hEVs from HFD animals and 77 EV markers exclusively present in control hEVs, with 10 EV markers shared between the two groups (Figure 3C and Tables S1 and S2). Subsequent analysis of the EV markers significantly modulated in HFD-treated animals

https://doi.org/10.1021/acsomega.5c02274
ACS Omega 2025, 10, 23563−23581

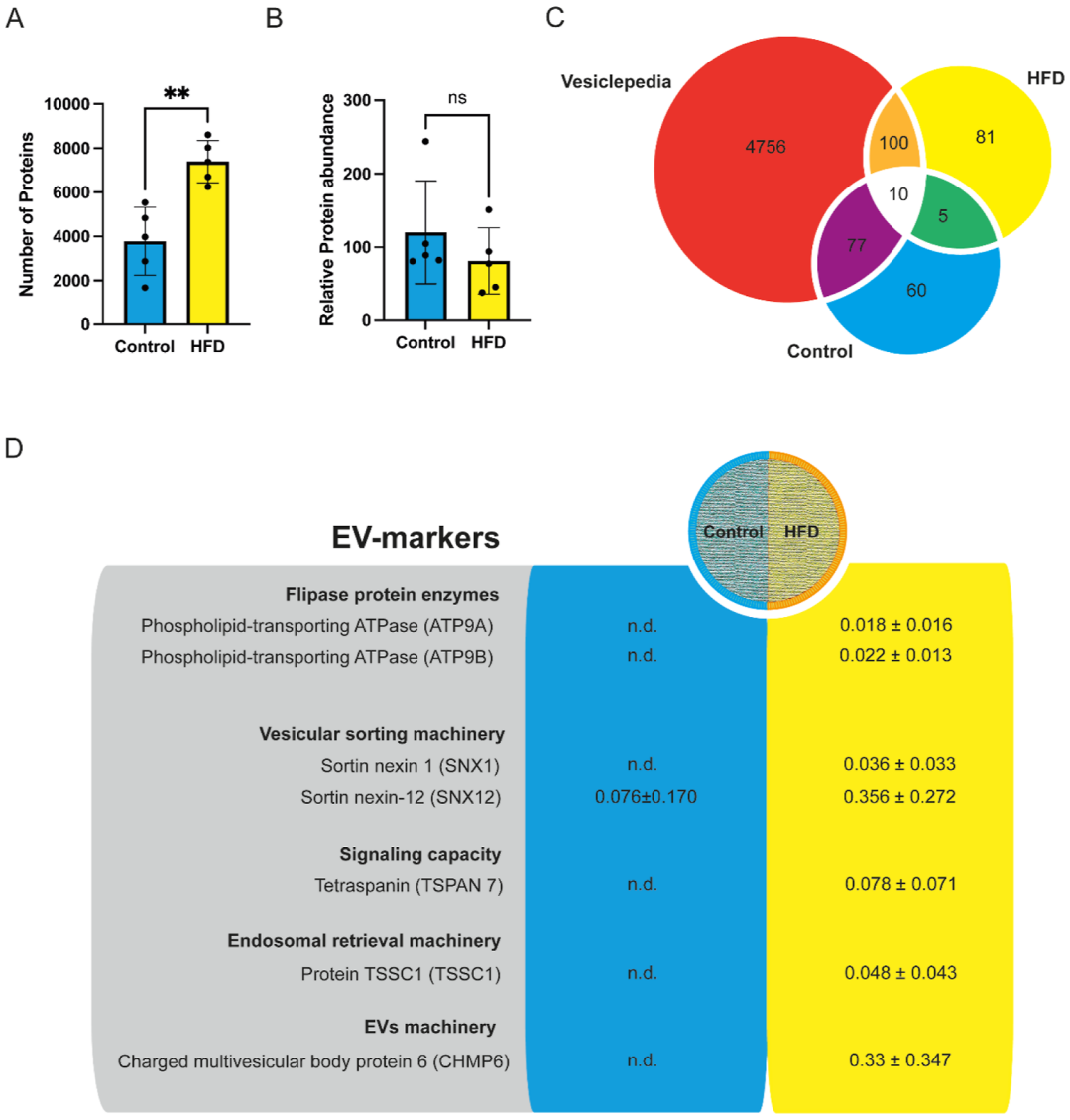

Figure 3. Proteomic profiling of hypothalamic extracellular vesicles (hEVs) (A) total number of proteins identified by liquid chromatography mass spectrometry proteomics in hEVs proteomes from Controls and high fat diet (HFD)-treated animals. (B) Relative protein quantitation based on sum of modified protein abundance index (emPAI) in hEVs from Controls and HFD-treated animals. Significant differences were assessed by student *t*-test. **indicates significant differences at $p \leq 0.01$. (C) Venn diagram representing the intersection between the proteins identified in hEVs proteomes from controls and HFD-treated animals from the database Vesiclepedia. (D) Proteins involved in EVs structure, sorting and cargo compositions detected in hEVs proteomes significantly upregulated in HFD animals compared to controls. Designations in bold within the panels indicate protein families. Protein abundance is expressed as emPAI. n.d. means not detected. Only proteins present in three or more biological replicates in a group and absent in four or more biological replicates in the other group were considered.

revealed several findings. Specifically, proteins such as phospholipid-transporting ATPase flippase enzymes, EV machinery-related proteins, vesicular sorting machinery-related proteins, endosomal retrieval machinery-related proteins, and EV signaling-related proteins were present in hEVs from HFD group (Figure 3D).

Exposure to HFD Overall Alters the Molecular Proteomes of hEVs. To investigate the modulation of hEVs proteomes in response to HFD exposure, we examined the subsets of hEVs proteins that were exclusively present or absent in HFD animals compared to controls (Data set S1 and S2). The identified subsets of proteins in the former analysis were further analyzed through pathway analysis to gain insights into the biological pathways affected by HFD exposure. The pathway analysis revealed notable differences in pathway representation between the two experimental groups as detected in hEVs (Figure 4A). In the control group (Figure 4A), the most enriched pathways included mRNA processing, which showed the highest number of pathway entities. Additional pathways prominently enriched involved oxidative stress and redox regulation, proteasome degradation, glutathione metabolism, and fatty acid beta-oxidation, reflecting a strong emphasis on cellular maintenance, metabolic regulation, and stress response.

In contrast, the HFD group (Figure 4A) exhibited a distinct pathway profile. While mRNA processing remained highly enriched, similar to the control group, the extent of pathway entity involvement was significantly reduced. Other pathways prominently enriched in the HFD group included oxidative phosphorylation, S1P receptor signal transduction, and apoptosis, indicating altered cellular signaling, and increased programmed cell death in response to the HFD. Additionally,

https://doi.org/10.1021/acsomega.5c02274
ACS Omega 2025, 10, 23563−23581

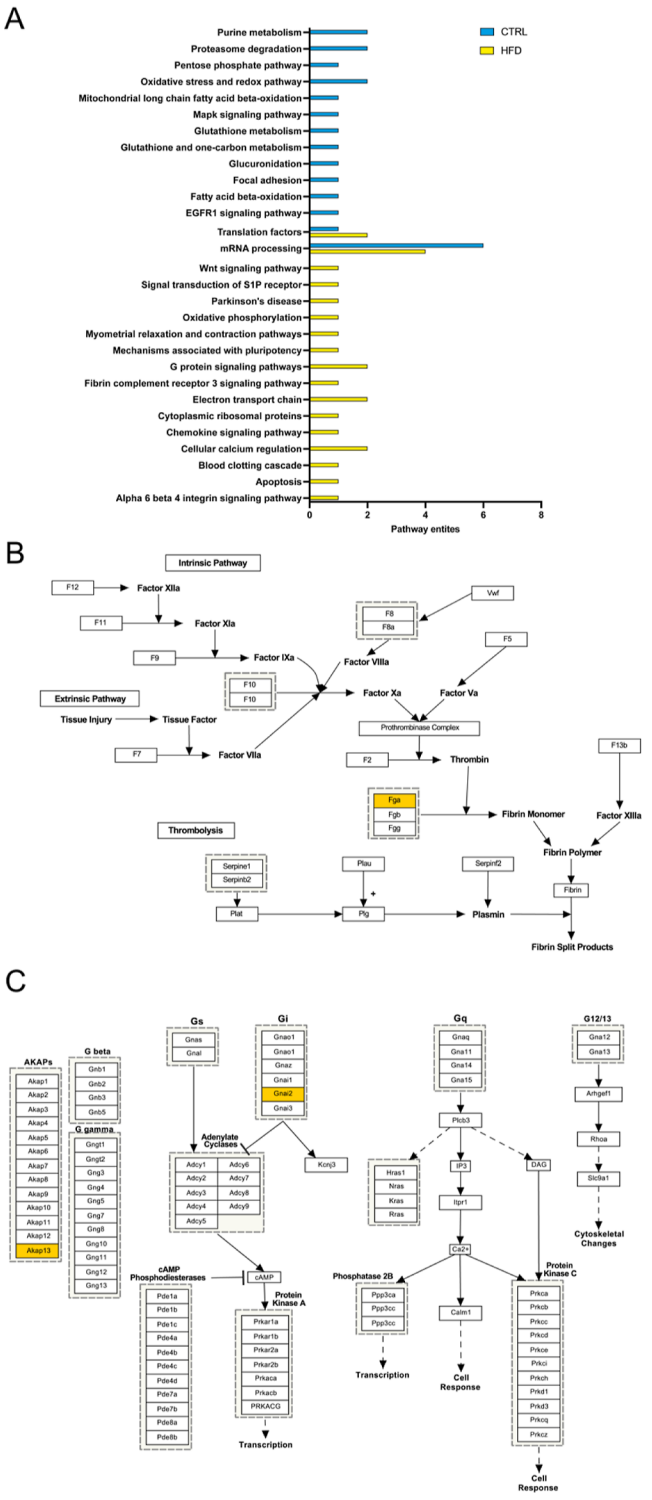

Figure 4. Pathway analysis of hypothalamic extracellular vesicle (hEV) proteomes from control animals (control) and high fat diet (HFD)-treated animals. (A) Pathways enriched in hEVs from Controls and HFD-animals. Only proteins present in three or more biological replicates in a group and absent in four or more biological replicates in the other group were considered. Representative examples of pathways modulated by HFD detectable in hEVs include (B). The blood clotting cascade pathway and (C) G-protein signaling pathway. Proteins from these specific pathways uniquely identified in hEVs of HFD-treated animals are represented in yellow boxes. Proteins uniquely identified in hEVs of control animals are represented in blue boxes.

pathways such as G protein signaling, focal adhesion, integrin signaling, and chemokine signaling were notably enriched, highlighting potential disruptions in cellular communication and immune responses in the hypothalamus under metabolic stress (Figure 4A).

To illustrate these findings further, we present a visual representation of three specific pathways where HFD-induced modulation of proteins was observed, including the blood clotting pathway (Figure 4B), G-protein signaling pathway (Figure 4C), and the mRNA processing pathway (Figure 5). Proteins modulated by HFD within these pathways are highlighted in yellow, emphasizing their critical roles in hypothalamic function under metabolic stress. Additionally, Table S3 provides further detail on the key biological functions and potential clinical relevance of the altered pathways identified.

Molecular Imprints of Liver Dysfunction and Lipid Metabolism in hEVs of HFD. Given that the establishment of the HFD-induced hamster model is characterized by early onset liver dysfunction and altered lipid metabolism, we independently evaluated whether the observed effects on hEV composition could be mechanistically linked to these model-specific alterations. Exposure to HFD induced significant alterations in the proteomic profiles of hEVs, particularly related to fatty acid metabolism and hepatic dysfunction (Table 1). Several proteins were exclusively detected in hEVs from HFD animals, including Aldehyde dehydrogenase, dimeric NADP-preferring protein (ALDH3A1) and Malic enzyme 1 (ME1). Their presence in hEVs derived from HFD-treated animals, but not in controls, suggests a reprogramming of fatty acid metabolic processes, likely as an adaptative response to excessive fat intake. In addition to proteins linked to fatty acid metabolism, the HFD group showed in hEVs upregulation of proteins associated with nonalcoholic fatty liver disease (NAFLD) and oxidative stress. Notably, both Hemoglobin subunit zeta (HBA-X) and Hemoglobin Z, beta-like embryonic chain (HBB-BH1) were significantly elevated in hEVs from HFD-exposed animals but were absent in controls. The release of hemoglobin is a known response to oxidative stress, and its detection in the hEVs likely reflect systemic disruptions in redox homeostasis induced by HFD exposure. These findings are consistent and provide novel molecular indicators of the hepatic dysfunction previously observed by us and other colleagues in HFD-hyperlipidemia models,[43,44] corroborated by autopsy and histopathological approaches.

Furthermore, the Ubiquinone biosynthesis protein (COQ9) and the Protein enabled homologue (ENAH), both associated with oxidative stress and inflammatory responses, were exclusively present in hEVs from HFD-treated animals reinforcing the idea of systemic inflammation and oxidative stress. Conversely, proteins involved in mitochondrial fatty acid oxidation, such as Alpha/beta hydrolase domain-containing protein 14A (ABHD14A), Short/branched-chain specific acyl-CoA dehydrogenase (ACADSB), and Trifunctional enzyme subunit alpha, mitochondrial (HADHA), were present in control hEVs but absent in those vesicles from HFD-exposed animals. This downregulation or loss in the HFD group points to an impairment in mitochondrial fatty acid oxidation.

hEV at the Onset of Obesity Display Singular Proteomic Compositions Linked to Obesity Comorbidities. *Molecular Imprints of Cancer.* HFD exposure led to the

https://doi.org/10.1021/acsomega.5c02274
ACS Omega 2025, 10, 23563−23581

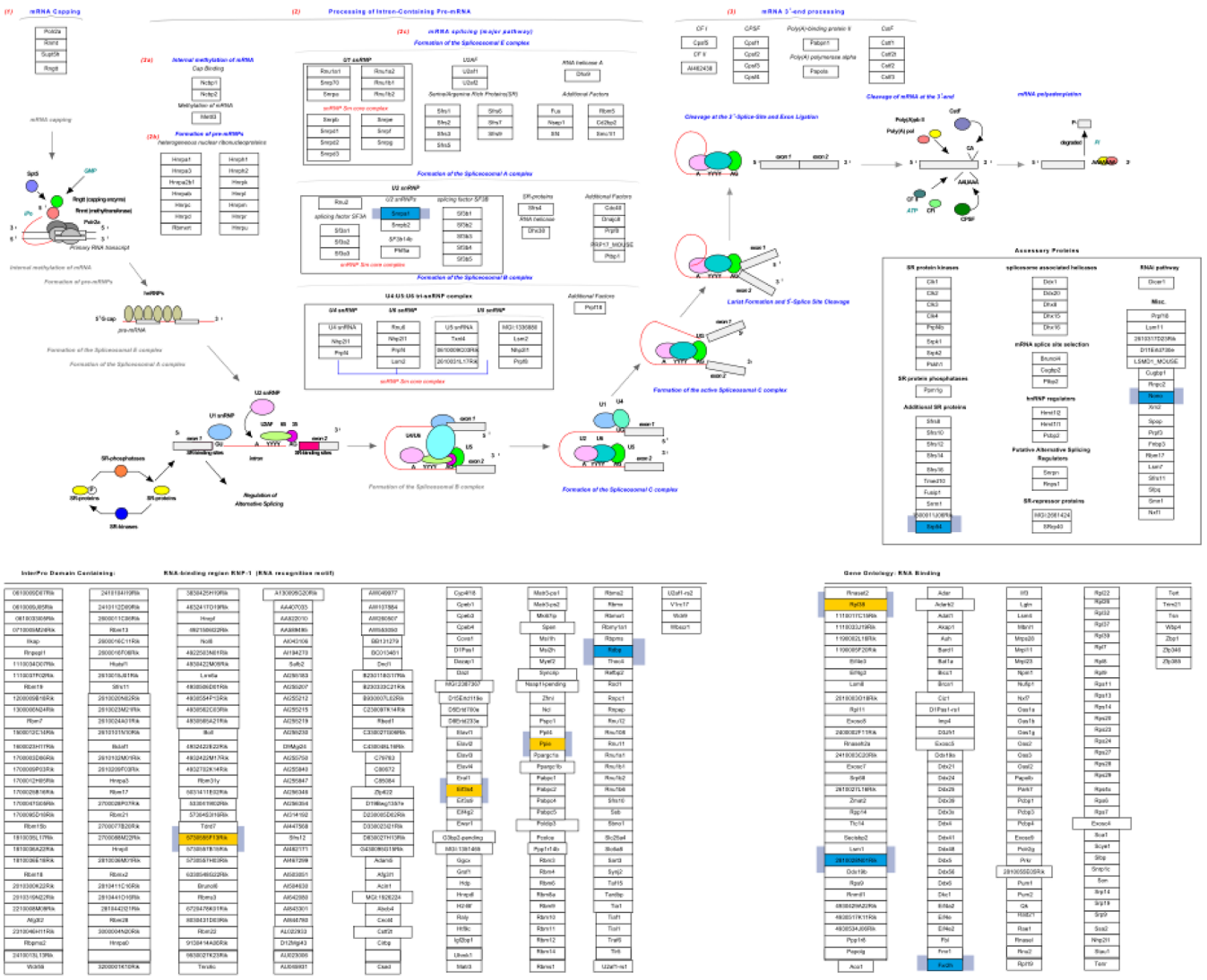

Figure 5. Representation of the mRNA processing pathway modulated by high fat diet (HFD) detectable in hypothalamic extracellular vesicle (hEV). Proteins uniquely identified in hEVs of HFD-treated animals are represented in yellow boxes. Proteins uniquely identified in hEVs of control animals are represented in blue boxes.

presence of proteins in hEVs that are associated with various obesity-related comorbidities, despite the absence of clinical signs of these comorbidities or significant increases in body weight at the time of autopsy (Figure 1B). Notably, the HFD triggered cellular processes implicated in cancer development and progression. The list of proteins related to cancer is provided in Table 2, with their potential roles in cancer development and progression annotated based on existing literature. Several proteins exclusively identified in hEVs from HFD-exposed animals are associated with oncogenesis, cell migration, and tumor aggressiveness. Among these, AKAP13 (AKAP13), Hepatoma-derived growth factor (HDGF) and NAD(P)H-hydrate epimerase (APOA1BP) were exclusively present in hEVs from the HFD group. Similarly, Actin-related protein 3B (ACTR3B) and Anaphase-promoting complex subunit 1(ANAPC1) were also enriched in this group. Furthermore, proteins such as the Isoform HMG-Y of high mobility group protein HMG-I/HMG-Y (HMGA1) and the eukaryotic translation initiation factor 3 subunit G (EIF4G3), both associated with tumorigenesis and progression in various cancers, were enriched in hEVs from the HFD group. Conversely, several cancer-suppressing proteins detected in control animals were absent in hEVs from HFD-exposed animals (Table 2), these included the Probable glutathione peroxidase 8 (GPX8) and Metastasis suppressor 1 (MTSS1). Additionally, key proteins such as Histone H2AX (H2AFX) and Trifunctional enzyme subunit alpha (HADHA) were also absent in the HFD group.

Molecular Imprints of Cardiovascular Diseases. Several proteins related to cardiovascular diseases (CVD) were identified in hEVs from animals subjected to a HFD (Table 3). Among these, Fetuin-A (AHSG), a protein involved in pro-inflammatory processes through TLR4 activation, and Fibrinogen Alpha (FGA) and Beta (FGB) chains were uniquely present in hEVs from animals exposed to HFD. Additionally, hEVs from HFD animals contained proteins implicated in vascular function and inflammation, such as Rho GTPase-activating protein 42 (ARHGAP42) and 14-3-3 protein sigma (SFN). Proteins involved in mitochondrial function, including the CDGSH iron−sulfur domain-containing protein 2 (CISD2), were also present in hEVs from the HFD-treated group. Conversely, several proteins that provide

https://doi.org/10.1021/acsomega.5c02274
ACS Omega 2025, 10, 23563−23581

Table 1. List of Present and Absent Proteins in Hypothalamic Extracellular Vesicles (hEVs) from Animals That Were Exposed to High Fat Diet (HFD) Associated to Fatty Acid Metabolism and Hepatic Dysfunction

protein description	gene symbol	emPAI[a] control	emPAI[a] HFD	role(s)	ref
Fatty Acid Metabolism					
HFD-Modulated Proteins Present in hEVs					
NADH dehydrogenase [ubiquinone] 1 alpha subcomplex subunit 3 Malic enzyme	NDUFA3	n.d.	0.222 ± 0.20	implicated in the correct mitochondrial assembly and energy metabolism	35
malic enzyme	ME1	n.d.	0.074 ± 0.084	role in NAPDH supply and the transfer of acetyl groups to the mitochondria	36
aldehyde dehydrogenase, dimeric NADP-preferring	ALDH3A1	n.d.[b]	0.040 ± 0.033	members of the family are upregulated after HFD exposure	37
HFD-Modulated Proteins Absent in hEVs					
alpha/beta hydrolase domain-containing protein 14A	ABHD14A	0.078 ± 0.072	n.d.	involved in lipid metabolism. Downregulation can impair lipid homeostasis, contributing to insulin resistance and development of DM	38
Hepatic Dysfunction					
HFD-Modulated Proteins Present in hEVs					
hemoglobin Z, beta-like embryonic chain	HBB-BH1	n.d.	0.460 ± 0.477	released by the liver in response to oxidative stress	39
hemoglobin subunit zeta	HBA-X	n.d.	0.390 ± 0.391	released by the liver in response to oxidative stress	40
protein enabled homologue	ENAH	n.d.	0.100 ± 0.141	associated with inflammatory diseases	40
ubiquinone biosynthesis protein COQ9, mitocondrial	COQ9	n.d.	0.090 ± 0.087	increased in response to oxidative stress	39
HFD-Modulated Proteins Absent in hEVs					
trifunctional enzyme subunit alpha, mitochondrial	HADHA	0.116 ± 0.071	n.d.	implicated in the oxidation of fatty acids in the mitochondria	41
short/branched chain-specific acyl-CoA dehydrogenase, mitochondrial	ACADSB	0.036 ± 0.033	n.d.	induces the decrease of fatty acid oxidation in NAFLD	42

[a]Abundance expressed as Exponentially Modified Protein Abundance Index (emPAI) for label-free relative quantitation. [b]n.d. means not detected. Only proteins present in three or more biological replicates in a group and absent in four or more biological replicates in the other were considered. Proteins are listed in each category in descending order of abundance according to emPAI-based relative quantification.

cardiovascular protection were absent in hEVs from HFD-treated animals. These include the mitochondrial ATP synthase F(0) complex subunit B1 (ATP5F1), and the Serine/threonine-protein kinase PAK2 (PAK2). The complete list of CVD-related proteins modulated in hEVs by HFD exposure is detailed in Table 3, with their potential roles annotated based on existing literature.

Molecular Imprints of Diabetes. The analysis of proteins linked to diabetes mellitus (DM) revealed significant alterations in hEVs from animals exposed to a HFD as detailed in Table 4. Several proteins involved in insulin metabolism were uniquely identified in hEVs from HFD animals. Among these, Insulin-degrading enzyme (IDE), a key player in glucose homeostasis, and Insulin-like growth factor-binding protein 7 (IGFBP7) were present. Proteins associated in cellular stress and apoptosis, such as Serine/threonine-protein kinase BRSK2 (BRSK2) and Beta-catenin-interacting protein 1 (CTNNBIP1) were also impacted by HFD. Additionally, calcium metabolism was notably affected, with proteins such as the voltage-dependent R-type calcium channel subunit alpha-1E (CACNA1E) and N-terminal EF-hand calcium-binding proteins (NECAB1 and NECAB2) appearing exclusively in HFD hEVs. Alterations in glycosylation processes, commonly associated with DM, were also observed. Specifically, Mannose-1-phosphate guanyltransferases alpha and beta (GMPPA and GMPPB) were uniquely detected in hEVs from HFD-treated animals.

Molecular Imprints of other Obesity Comorbidities. In addition to the aforementioned obesity comorbidities, other molecular alterations were observed in hEVs from animals exposed to HFD, potentially associated with conditions such as kidney dysfunction, oxidative stress, and other obesity-related complications (Table 5). Proteins uniquely present in hEVs from HFD animals included Granzyme B (GZMB), linked to pro-inflammatory processes, and Apoptotic chromatin condensation inducer in the nucleus (ACIN1), associated with apoptosis. Additionally, C-terminal binding protein 2 (CTBP2), which regulates fat-selective gene programs, and FAS-associated factor 2 (FAF2), involved in protein degradation, were also modulated by HFD exposure.

Notably, several protective proteins involved in oxidative stress response and cardiovascular health were absent in hEVs from HFD-treated animals. These included Redox-regulatory protein FAM213A (FAM213A), Glucose-6-phosphate 1-dehydrogenase X (G6PDX), and Peroxiredoxin-5 (PRDX5), suggesting a loss of antioxidant defense mechanisms under HFD conditions.

Interaction Network Analysis of Proteins in hEVs from HFD-Treated Animals. We performed a protein−protein interaction (PPI) analysis using the STRING database, incorporating all proteins identified as differentially regulated in hEVs from HFD-fed animals compared to controls (listed in Tables 1−5). The resulting interaction network demonstrated extensive connectivity among these proteins (Figure 6). Central hub proteins were identified, notably SRC (Proto-oncogene tyrosine-protein kinase Src), a kinase involved in oncogenic signaling and cell migration, which exhibited interactions with multiple proteins, including FGB (Fibrinogen beta chain), a coagulation factor associated with cerebrovascular and metabolic disorders. These findings suggest that

https://doi.org/10.1021/acsomega.5c02274
ACS Omega 2025, 10, 23563−23581

Table 2. List of Present and Absent Proteins in Hypothalamic Extracellular Vesicles (hEVs) from Animals That Were Exposed to High Fat Diet (HFD) Associated Cancer[c]

protein description	gene symbol	emPAI[a] control	emPAI[a] HFD	role(s)	ref
HFD-Modulated Proteins Present in hEVs					
prothymosin alpha (Fragment)	PTMA	n.d.	0.456 ± 0.582	poor prognosis marker of hepatocellular carcinoma	45
programmed cell death protein 10 (Fragment)	PDCD10	n.d.	0.420 ± 0.471	dual role in tumorogenesis and migration	46
transmembrane protein 72	TMEM72	n.d.	0.408 ± 0.228	implicated in the dysregulation of phosphorilated proteins involved in MAPK or TLRs activity	47
isoform HMG-Y of high mobility group protein HMG-I/HMG-Y	HMGA1	n.d.	0.392 ± 0.543	potential biomarker in thyroid related tumors	48
40S ribosomal protein S7	RPS7	n.d.	0.246 ± 0.316	increases cell invasion	49
hepatoma-derived growth factor (fragment)	HDGF	n.d.	0.200 ± 0.162	constitutes a growth-promoting factor of cancer cells	50
NAD(P)H-hydrate epimerase	APOA1BP	n.d.	0.142 ± 0.202	participates in cancer proliferation	51
thioredoxin-related transmembrane protein 1 (fragment)	TMX1	n.d.	0.132 ± 0.098	modulatory role over SERCAs modulating mitochondrial activity	52
actin-related protein 3B	ACTR3B	n.d.	0.116 ± 0.124	its dimerization with Arp2 promotes migration pathways in different types of cancer	53
protein Srsf11	SRSF11	n.d.	0.112 ± 0.153	mutations are reported in multiple cancers	54
tyrosine-protein kinase	SRC	n.d.	0.112 ± 0.077	impact in metastasis	55
Eukaryotic translation initiation factor 3 subunit G	EIF3G	n.d.	0.094 ± 0.095	subunit G is reported to be related to osteosarcoma	56
tetraspanin	TSPAN7	n.d.	0.078 ± 0.071	increases proliferation and migration	57
nectin-1	PVRL1	n.d.	0.072 ± 0.066	upregulated blocks the infiltration of antitumoral immune cells	58
regulator of G-protein-signaling 6	RGS6	n.d.	0.064 ± 0.065	act as a tumor suppressor by inducing apoptosis	59
E3 ubiquitin-protein ligase RNF126	RNF126	n.d.	0.060 ± 0.054	blocks the action of p21, inducing cell growth	60
membrane-associated guanylate kinase, WW and PDZ domain-containing protein 2	MAGI2	n.d.	0.054 ± 0.077	related to tumor agresiveness	61
Olfactory receptor 51E2	OR51 × 10^2	n.d.	0.054 ± 0.049	melanoma detection marker	62
Protein arginine *N*-methyltransferase 5	PRMT5	n.d.	0.050 ± 0.022	widely studied as therapeutic target due to its interaction withp53-derived factors	63
Threonine-tRNA ligase, cytoplasmic	TARS	n.d.	0.040 ± 0.028	predictive marker for cancer survival	64
late secretory pathway protein AVL9 homologue	AVL9	n.d.	0.038 ± 0.038	participates in cell migration	65
cleavage and polyadenylation-specificity factor subunit 6	CPSF6	n.d.	0.036 ± 0.033	regulated by phosphorilation enabling its nuclear importation and enhancing polyadenylation	66
spermatid perinuclear RNA-binding protein	STRBP	n.d.	0.024 ± 0.022	can interact with Dicer promoting the degradation of miRNAs linked to cancer development	67
Eukaryotic translation initiation factor 4 gamma 3	EIF4G3	n.d.	0.022 ± 0.022	derived circular RNA associated with its gene can be a marker of hepatocellular carcinoma	68
phosphatidylinositol 3-kinase	PIK3C3	n.d.	0.020 ± 0.018	mutations or aberrant amplifications in their sequence are reported in several types of cancer	69
isoform 2 of Teneurin-3	TENM3	n.d.	0.018 ± 0.029	drive malignancy and metastasis in several tumors	70
breakpoint cluster region protein	BCR	n.d.	0.018 ± 0.020	induces different types of neoplasia related to red and white cells	71
transforming acidic coiled-coil-containing protein 2	TACC2	n.d.	0.018 ± 0.020	upregulated in patients with bad prognosis breast cancer	72
receptor-type tyrosine-protein phosphatase S	PTPRS	n.d.	0.016 ± 0.017	known are mutated in different types of cancer	73
structural maintenance of chromosomes protein	SMC3	n.d.	0.016 ± 0.009	regulates apoptotic activity	74
protein Akap13	AKAP13	n.d.[b]	0.008 ± 0.008	marker of bad prognosis in hepatocellular carcinomas	75
anaphase-promoting complex subunit 1	ANAPC1	n.d.	0.008 ± 0.008	the APC complex upregulation is related to the loss of checkpoint regulation in cell cycle	76
HFD-Modulated Proteins Absent in hEVs					
histone H2AX	H2AFX	23.726 ± 29.619	n.d.	linked to oxidative stress initiated cell death	77
RAB3B, member RAS oncogene family, isoform CRA_a	RAB3B	0.138 ± 0.140	n.d.	linked to the effects of dietary iron in adipose tissue and glucose metabolism	78
trifunctional enzyme subunit alpha, mitochondrial	HADHA	0.116 ± 0.071	n.d.	downregulation is related to cell migration and invasion	79
Rho GTPase-activating protein 1	ARHGAP1	0.108 ± 0.128	n.d.	important role in p53 regulation	80
probable glutathione peroxidase 8	GPX8	0.084 ± 0.077	n.d.	implicated in inhibiting tumor cell migration	81
MTSS1-like protein	MTSS1L	0.046 ± 0.053	n.d.	marker of prognosis of gastic cancer patients	82
short/branched chain-specific acyl-CoA dehydrogenase, mitochondrial	ACADSB	0.036 ± 0.033	n.d.	downregulation is correlated to cancer prognosis	83
cadherin-11	CDH11	0.032 ± 0.033	n.d.	modulates cell adhesion capacities	84

https://doi.org/10.1021/acsomega.5c02274
ACS Omega 2025, 10, 23563−23581

Table 2. continued

protein description	gene symbol	emPAI[a] control	emPAI[a] HFD	role(s)	ref
HFD-Modulated Proteins Absent in hEVs					
26S proteasome non-ATPase regulatory subunit 3	PSMD3	0.030 ± 0.027	n.d.	downregulation in high survival patients	85
metastasis suppressor 1, isoform CRA_e	MTSS1	0.024 ± 0.053	n.d.	marker of prognosis of gastic cancer patients	82

[a]Abundance expressed as Exponentially Modified Protein Abundance Index (emPAI) for label-free relative quantitation. [b]n.d. means not detected. Only proteins present in three or more biological replicates in a group and absent in four or more biological replicates in the other were considered. Proteins are listed in each category in descending order of abundance according to emPAI-based relative quantification. [c]Presence was considered when the protein was identified in four or more biological replicates in a group.

Table 3. List of Present and Absent Proteins in Hypothalamic Extracellular Vesicles (hEVs) from Animals That Were Exposed to High Fat Diet (HFD) Associated with Cerebrovascular Disease (CVD)[c]

protein description	gene symbol	emPAI[a] control	emPAI[a] HFD	role(s)	ref
HFD-Modulated Proteins Present in hEVs					
14-3-3 protein sigma	SFN	n.d.	0.350 ± 0.340	Role in vascular inflammations	86
Endothelial differentiation-related factor 1	EDF1	n.d.	0.180 ± 0.190	Phosphorilated bounds calmodulin which can increase the generation of nitric oxide	87
Alpha-2-HS-glycoprotein	AHSG	n.d.[b]	0.070 ± 0.075	Influence in the secretion of pro-inflammatory factors	88
Hyaluronan and proteoglycan link protein 4	HAPLN4	n.d.	0.060 ± 0.067	Implicated in synaptogenesis	89
Sodium/hydrogen exchanger	SLC9A1	n.d.	0.050 ± 0.040	Implicated in Na and H reperfusion during endothelial dysfunction	90
Fibrinogen beta chain	FGB	n.d.	0.040 ± 0.033	Upregulation increases the risk of dementia Upregulation increases the risk of dementia	91
Fibrinogen alpha chain	FGA	n.d.	0.030 ± 0.033		
Bifunctional glutamate/proline-tRNA ligase	EPRS	n.d.	0.030 ± 0.018	Role in inflammatory processes	92
Isoform 2 of Angiomotin-like protein 1	AMOTL1	n.d.	0.020 ± 0.016	Implicated in vessel sprouting	93
Rho GTPase-activating protein 42	ARHGAP42	n.d.	0.020 ± 0.016	Influence blood pressure	94
Formin-like 1, isoform CRA_c	FMNL1	n.d.	0.020 ± 0.016	Bleb formation of the membrane which induces interactions with inflammatory factors	95
HFD-Modulated Proteins Absent in hEVs					
CDGSH iron–sulfur domain-containing protein 2	CISD2	0.598 ± 0.701	n.d.	Linked to mitochondrial function	96
Serine/threonine-protein kinase PAK	PAK2	0.252 ± 0.242	n.d.	Dysregulation linked to cardiac function	97
Mitochondrial 2-oxoglutarate/malate carrier protein (Fragment)	SLC25A11	0.168 ± 0.170	n.d.	Involved in mitochondrial function	98
ATP synthase F(0) complex subunit B1, mitochondrial	ATP5F1	0.120 ± 0.155	n.d.	Subunit of ATP synthase; mitochondrial dysfunction is linked to CVD	99
Protein kinase C	PRKCG	0.072 ± 0.054	n.d.	Dysregulation linked to CVD	100
Adenosine kinase	ADK	0.048 ± 0.044	n.d.	Involved in adenosine metabolism (cardioprotective effects)	101
Isoform 3 of Sorbin and SH3 domain-containing protein 2	SORBS2	0.032 ± 0.034	n.d.	Involved in cardiac stress signaling	102

[a]Abundance expressed as Exponentially Modified Protein Abundance Index (emPAI) for label-free relative quantitation. [b]n.d. means not detected. Only proteins present in three or more biological replicates in a group and absent in four or more biological replicates in the other were considered. Proteins are listed in each category in descending order of abundance according to emPAI-based relative quantification. [c]Presence was considered when the protein was identified in four or more biological replicates in a group.

diverse biological processes—such as inflammation, metabolism, vascular integrity, and cellular signaling—converge in potential PPIs within extracellular vesicles during the initial stages of obesogenic stress.

DISCUSSION

This investigation provides relevant insights into the molecular modulations of hEVs induced by 30 day HFD exposure at the onset of obesity, a stage characterized by leptin signaling disruption. These findings reinforce the central role of the hypothalamus in metabolic regulation and its susceptibility to dietary challenges. Syrian golden hamsters were selected as a model of onset of obesity for their lipoprotein metabolism, which closely resembles that of humans.[133] This model develops hepatic steatosis without transaminase alterations and exhibits changes in lysophospholipid composition after 30 days of HFD exposure, as previously reported.[43,44,134] Importantly, the presence of elevated plasma leptin levels and impaired leptin signaling confirms the utility of this model for studying early events in diet-induced obesity.

Furthermore, the findings presented herein underscore the potential of EVs as biomarkers and mediators, shedding light on critical molecular alterations linked to obesity comorbidities even before their clinical manifestation. The hypothalamus integrates signals related to nutrient status, inflammation, and energy expenditure. Proteomic changes in this region can

https://doi.org/10.1021/acsomega.5c02274
ACS Omega 2025, 10, 23563−23581

Table 4. List of Present and Absent Proteins in Hypothalamic Extracellular Vesicles (hEVs) from Animals That Were Exposed to High Fat Diet (HFD) Associated to DM[c]

protein description	gene symbol	emPAI[a] control	emPAI[a] HFD	role(s)	ref
HFD-Modulated Proteins Present in hEVs					
Beta-catenin-interacting protein 1	CTNNBIP1	n.d.[b]	0.950 ± 0.990	Modulates the susceptibility to DM	103
Protein S100	S100A1	n.d.	0.280 ± 0.313	Related to the presence of an oxidative stress in DM	104
Actin-related protein 3B	ACTR3B	n.d.	0.120 ± 0.124	Upregulated in childhood obesity	53
Insulin-like growth factor-binding protein 7	IGFBP7	n.d.	0.090 ± 0.095	Associated with insulin resistance	105
Mannose-1-phosphate guanyltransferase beta	GMPPB	n.d.	0.070 ± 0.070	Correlated with increased glycosylation in DM and endothelial dysfunction	106
N-terminal EF-hand calcium-binding protein 2	NECAB2	n.d.	0.070 ± 0.065	It is involved in ER stress (a hallmark of type 2 DM)	107
N-terminal EF-hand calcium-binding protein 1	NECAB1	n.d.	0.070 ± 0.070	Elevated in pancreatic cells in DM as a consequence of an insulin secretion impairment	108
Tyrosine-protein kinase	MATK	n.d.	0.060 ± 0.073	Involved in glucose metabolism and insult sensitivity	109
Mannose-1-phosphate guanyltransferase alpha	GMPPA	n.d.	0.060 ± 0.031	Correlated with increased glycosylation in DM and endothelial dysfunction	106
Serine/threonine-protein kinase BRSK2	BRSK2	n.d.	0.040 ± 0.053	Upregulation induces apoptosis	110
Transketolase-like protein 1	TKTL1	n.d.	0.040 ± 0.042	Its function is impeded in DM	111
Regulator of microtubule dynamics protein 3	RMDN3	n.d.	0.040 ± 0.032	Associated to the regulation of blood glucose	112
Insulin-degrading enzyme (Fragment)	IDE	n.d.	0.020 ± 0.025	Implicated in glucose homeostasis	113
Calcium-binding and coiled-coil domain-containing protein 1	CALCOCO1	n.d.	0.020 ± 0.022	Calcium channels activation is dependent on dietary requirements	114
PERQ amino acid-rich with GYF domain-containing protein 1	GIGYF1	n.d.	0.020 ± 0.016	Involved in the regulation of insulin receptors	115
Voltage-dependent R-type calcium channel subunit alpha-1E	CACNA1E	n.d.	0.010 ± 0.005	Associated to type 2 diabete and insulin secretion	116
Ryanodine receptor 2	RYR2	n.d.	0.010 ± 0.005	Impaired in islets from diabetic patients	117
HFD-Modulated Proteins Absent in hEVs					
Hepatoma-derived growth factor-related protein 3	HDGFRP3	0.224 ± 0.165	n.d.	Downregulation is linked to obesity and related complications, including type 2 DM and NAFLD	118
Phosphoglucomutase-2	PGM2	0.194 ± 0.256	n.d.	Involved in glycogen metabolism	119
Guanine nucleotide-binding protein G(q) subunit alpha	GNAQ	0.118 ± 0.146	n.d.	Dysregulation is linked to obesity-related insulin resistance	120
MCG49978	PLCXD3	0.116 ± 0.129	n.d.	Involved in regulation of insulin sensitivity.	121
GMP reductase 1 (Fragment)	GMPR	0.108 ± 0.143	n.d.	Downregulation impact glucose metabolism and insulin sensitivity	122
Methylcrotonoyl-CoA carboxylase subunit alpha	MCCC1	0.024 ± 0.022	n.d.	Downregulation impairs amino acid catabolism, leading to metabolic disturbances associated with insulin resistance and type 2 DM	123
T-cell lymphoma invasion and metastasis 1	TIAM1	0.012 ± 0.011	n.d.	Downregulation linked to obesity-related inflammation and insulin resistance	124

[a]Abundance expressed as Exponentially Modified Protein Abundance Index (emPAI) for label-free relative quantitation. [b]n.d. means not detected. Only proteins present in three or more biological replicates in a group and absent in four or more biological replicates in the other were considered. Proteins are listed in each category in descending order of abundance according to emPAI-based relative quantification. [c]Presence was considered when the protein was identified in four or more biological replicates in a group.

initiate cascading effects that promote pathogenic events and alter the proteome.[135−137] Short-term high fat consumption (3 days) has been shown to cause rapid proteomic changes linked to cellular stress and altered synaptic plasticity.[138] Similarly, this study highlights proteomic changes in hEVs from HFD-exposed hamsters, pointing to early disruptions in pathways critical to maintaining metabolic homeostasis, including lipid metabolism, oxidative stress, and cell signaling.[139,140]

Our findings demonstrate that, in contrast to previous studies that primarily analyzed circulating EVs derived from specific obesity-affected organs, hEVs offer a broader perspective on obesity-associated complications. This observation aligns with previously reported roles of extracellular vesicles in reflecting and promoting obesity-related comorbidities. For example, Povero et al. illustrated the biomarker potential of circulating EVs for detecting liver injury in experimental fatty liver disease.[141] Additionally, the involvement of organ-specific EVs in facilitating metastasis across various obesity-related cancers has been extensively reported.[142,143]

One of the most noteworthy outcomes of this study is thus the identification of proteins in hEVs that are associated with the development of obesity-related comorbidities, including cardiovascular disease, cancer, and kidney dysfunction, at the

https://doi.org/10.1021/acsomega.5c02274
ACS Omega 2025, 10, 23563−23581

Table 5. List of Present and Absent Proteins in Hypothalamic Extracellular Vesicles (hEVs) from Animals That Were Exposed to High Fat Diet (HFD) Associated to Apoptosis, Oxidative Stress, Brown/White Fat Homeostasis and Proteasome Activity[a]

protein description	gene symbol	emPAI[a] control	emPAI[a] HFD	role(s)	ref
Apoptosis					
HFD-Modulated Proteins Present in hEVs					
SAFB-like transcription modulator	SLTM	n.d.	0.020 ± 0.016	Upregulated inhibit transcription	125
Granzyme B	GZMB	n.d.	0.018 ± 0.017	Pro-inflammatory	126
Apoptotic chromatin condensation inducer in the nucleus (Fragment)	ACIN1	n.d.	0.010 ± 0.011	Role in induction of apoptotic chromatin condensation	127
Oxidative Stress					
HFD-Modulated Proteins Absent in hEVs					
Peroxiredoxin-5, mitochondrial	PRDX5	0.238 ± 0.066	n.d.	Antioxidant enzyme	128
Redox-regulatory protein FAM213A	FAM213A	0.078 ± 0.071	n.d.	Involved in oxidative stress response	129
Glucose-6-phosphate 1-dehydrogenase X	G6PDX	0.042 ± 0.045	n.d.	Deficiency increases oxidative stress in inflammatory conditions	130
Brown/White Fat Homeostasis					
HFD-Modulated Proteins Present in hEVs					
C-terminal binding protein 2, isoform CRA_b	CTBP2	n.d.	0.090 ± 0.177	Involved in brown and white fat-selective gene programs	131
Proteasome Activity					
HFD-Modulated Proteins Present in hEVs					
FAS-associated factor 2 (Fragment)	FAF2	n.d.	0.130 ± 0.175	Involved in translocation of terminally misfolded proteins	132

[a]Presence was considered when the protein was identified in four or more biological replicates in a group. Absence (n.d.) was considered when the protein was not identified in 4 animals or more. Proteins are listed in each category in descending order of abundance according to emPAI-based relative quantification.

onset of obesity. Remarkably, these changes occurred in the absence of significant weight gain or clinical signs of these conditions. For instance, the detection of oncogenic proteins such as AKAP13 and ACTR3B in hEVs suggests that HFD may create a pro-tumorigenic environment early in the disease process.[144−146] Similarly, the presence of fibrinogen chains, key components in blood clotting, indicates an increased risk of cardiovascular complications linked to hypothalamic dysregulation.[147,148] The detection of insulin-related proteins in hEVs from HFD treated animals, such as IDE, suggests early disruption in glucose metabolism and insulin signaling. Upregulation of IDE in the central nervous system has been linked to excessive insulin degradation, impairing neuronal insulin signaling pathways. This impairment is associated with reduced synaptic plasticity, a critical factor for learning and memory,[149] and represents a significant pathological alteration, particularly relevant in the context of childhood obesity. similarly, our data is consistent with previous findings that identified a crucial role of the mitochondrial and endoplasmic reticulum proteomes on the homeostasis of hypothalamic neurons under leptin resistance conditions.

Classic obesity biomarkers, such as anthropometric, biochemical, hormonal, and molecular markers, including the monitoring of altered serum glucose, HbA1c, and lipid profiles, are well-established indicators association with obesity.[150] In addition, more specific molecular changes linked to obesity can be detected. For instance, adipokines, cytokines secreted by adipose tissue, play a key role in the development of obesity-related metabolic disorders and CVD.[151] However, while classic obesity biomarkers provide useful insights into metabolic disturbances and current comorbidities, they have limitations in predicting the future risk of developing these conditions. Their levels can be influenced by transient factors such as diet, stress, or medication, and they may fail to fully capture the complexity of obesity-related pathophysiology. Similarly, obesity has been shown to influence the onset of several chronic diseases, including cancer, neurodegenerative disorders, and cardiovascular disease.[152] Our findings at the initial stage of the obesogenic insult suggest several mechanisms through which prolonged exposure may contribute to the development and progression of these major conditions—a hypothesis that warrants further investigation.

EVs play a significant role in the pathophysiology of obesity, acting as mediators of cellular communication and influencing metabolic processes. These vesicles regulate both central and peripheral signals that govern obesity.[153,154] The detailed characterization of hEVs at the onset of obesity after short-term HFD exposure provides clear evidence of obesity-associated pathological events in the animal model, including liver impairment and disrupted lipid metabolism. Notably, these small vesicles offer integrated and systemic insights into potential obesity-related complications, given their ability to circulate throughout the body.[31] This information could prove critical for the early detection of obesity-associated sequelae, especially considering the systemic nature of EVs. However, the clinical translation of findings from animal models must be carefully considered, and future clinical studies will be essential to comprehensively evaluate the potential of brain-derived circulating EVs as biomarkers for obesity-related comorbidities in both extended preclinical and clinical settings.

CONCLUSIONS

This study highlights the critical role of the hypothalamus in obesity and the significant molecular information embedded within EVs. Due to their inherent ability to circulate and cross biological barriers, EVs offer a unique opportunity as biomarkers and potential mediators of metabolic dysfunction. Our findings demonstrate that hEVs can detect early molecular

https://doi.org/10.1021/acsomega.5c02274
ACS Omega 2025, 10, 23563−23581

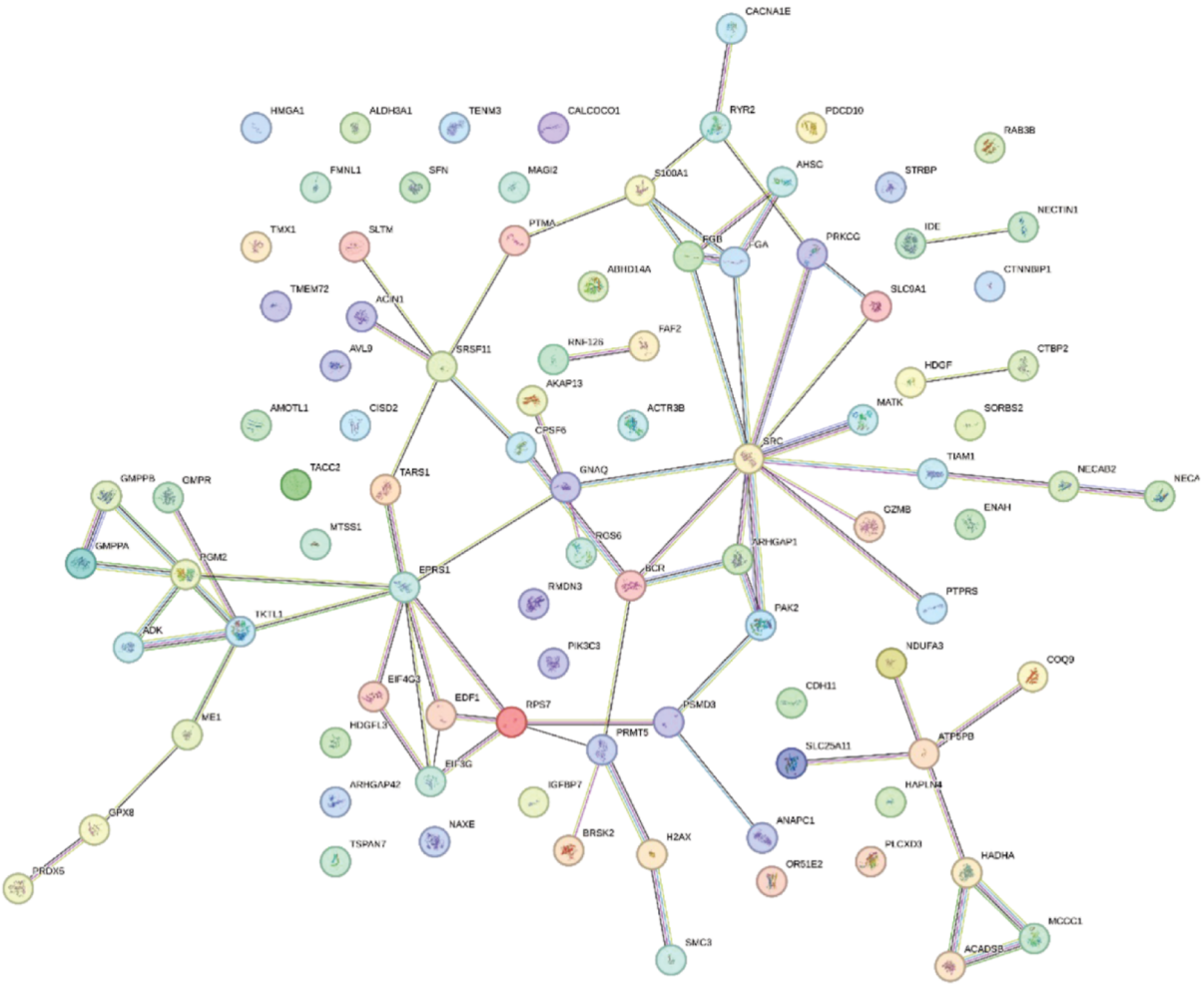

Figure 6. Protein−protein interaction (PPI) network of proteins modulated in hypothalamic extracellular vesicles (hEVs) from animals exposed to high fat diet (HFD). The network was generated using STRING. Each node represents a proteins, and edges indicate predicted or experimentally validated associations. Edge colors correspond to interaction types: Known interactions: light blue (curated databases), pink (experimentally determined); Predicted interactions: green (gene neighborhood), red (gene fusions), dark blue (gene co-occurrence); others: yellow (text mining), black (coexpression), light purple (protein homology).

changes preceding clinical comorbidities, presenting a promising approach for early diagnosis and intervention in obesity-related diseases. These insights emphasize the value of hEVs in unraveling the molecular underpinnings of obesity and its associated complications. Future research should prioritize detailed functional characterization of these proteomic alterations and explore clinical applications of hEVs for preventing and managing obesity and its comorbidities.

LIMITATIONS OF THE STUDY

While this study provides novel insights into the molecular changes in hypothalamic extracellular vesicles (hEVs) during the onset of obesity, it is not without limitations. First, the use of a Syrian hamster model, although relevant due to its similarities to human lipoprotein metabolism, may not fully capture the complexity of human obesity and its comorbidities. Second, the study focuses on a short-term high fat diet (HFD) exposure, limiting the ability to assess long-term adaptations and progression of obesity-related disorders. Finally, further validation in clinical samples is needed to confirm their circulation ability in bodily fluids and the translational potential of the identified hEV biomarkers for human obesity and its associated comorbidities. Future studies should address these limitations by incorporating longitudinal designs and integrating multiomics approaches.

ASSOCIATED CONTENT

Data Availability Statement

All data reported in this paper, including proteomic data sets and pathway analyses, have been made publicly available through the PRIDE repository under the identifier PXD058280. Access during the review process can be obtained with the following login details: Username: reviewer_pxd058280@ebi.ac.uk Password: CqukXuBdpSVm

Supporting Information

The Supporting Information is available free of charge at https://pubs.acs.org/doi/10.1021/acsomega.5c02274.

Proteins from Top-100 EV markers of Vesiclepedia present in hypothalamic extracellular vesicles (hEVs) from control animals (C) identified by LC−MS/MS (Table S1) (DOCX) proteins from Top-100 EV markers of Vesiclepedia present in hypothalamic extracellular vesicles (hEVs) from high fat diet animals (HFD) identified by LC−MS/MS (Table S2). Detailed description of the major biological functions and

https://doi.org/10.1021/acsomega.5c02274
ACS Omega 2025, 10, 23563−23581

potential clinical implication of the pathways identified contained dysregulated proteins in HFD animals compared to controls (Table S3) (PDF)

List of proteins identified by LC−MS/MS in control (C) animals and HFD-treated animals that pass the unique protein criteria of being identified in three or more biological replicates in the C group and absent in four or more biological replicates in the HFD group (Data set S1) (XLSX)

List of proteins identified by LC−MS/MS in high fat diet-treated animals (HFD) and control animals that pass the unique protein criteria of being identified in three or more biological replicates in the HFD group and absent in four or more biological replicates in the C group (Data set S2) (XLSX)

AUTHOR INFORMATION

Corresponding Authors

Xavier Gallart-Palau − *Biomedical Research Institute of Lleida Dr. Pifarré Foundation (IRBLLEIDA)—+Pec Proteomics Research Group (+PPRG)—Neuroscience Area, University Hospital Arnau de Vilanova (HUAV), 25198 Lleida, Catalonia, Spain; Department of Medical Basic Sciences (UdL)—Biomedical Research Institute of Lleida Dr. Pifarré Foundation (IRBLLEIDA), +Pec Proteomics Research Group (+PPRG), University of Lleida, 25198 Lleida, Catalonia, Spain;* orcid.org/0000-0001-5160-8794; Email: xgallart@irblleida.cat

Aida Serra − *Biomedical Research Institute of Lleida Dr. Pifarré Foundation (IRBLLEIDA)—+Pec Proteomics Research Group (+PPRG)—Neuroscience Area, University Hospital Arnau de Vilanova (HUAV), 25198 Lleida, Catalonia, Spain; Department of Medical Basic Sciences (UdL)—Biomedical Research Institute of Lleida Dr. Pifarré Foundation (IRBLLEIDA), +Pec Proteomics Research Group (+PPRG), University of Lleida, 25198 Lleida, Catalonia, Spain*; Email: aida.serra@udl.cat

Authors

María Fernández-Rhodes − *Biomedical Research Institute of Lleida Dr. Pifarré Foundation (IRBLLEIDA)—+Pec Proteomics Research Group (+PPRG)—Neuroscience Area, University Hospital Arnau de Vilanova (HUAV), 25198 Lleida, Catalonia, Spain; Department of Medical Basic Sciences (UdL)—Biomedical Research Institute of Lleida Dr. Pifarré Foundation (IRBLLEIDA), +Pec Proteomics Research Group (+PPRG), University of Lleida, 25198 Lleida, Catalonia, Spain*

Manuel Suárez − *Departament de Bioquímica i Biotecnologia, Nutrigenomics Research Group, Universitat Rovira i Virgili, 43007 Tarragona, Spain; Institut d'Investigació Sanitària Pere Virgili, Nutrigenomics Research Group, Universitat Rovira i Virgili, 43007 Tarragona, Spain; Center of Environmental, Food and Toxicological Technology (TecnATox), Nutrigenomics Research Group, University Rovira i Virgili, 43007 Tarragona, Spain;* orcid.org/0000-0003-0122-8253

Itziar Molet − *Biomedical Research Institute of Lleida Dr. Pifarré Foundation (IRBLLEIDA)—+Pec Proteomics Research Group (+PPRG)—Neuroscience Area, University Hospital Arnau de Vilanova (HUAV), 25198 Lleida, Catalonia, Spain; Department of Medical Basic Sciences (UdL)—Biomedical Research Institute of Lleida Dr. Pifarré Foundation (IRBLLEIDA), +Pec Proteomics Research Group (+PPRG), University of Lleida, 25198 Lleida, Catalonia, Spain*

Susana Suárez-García − *Departament de Bioquímica i Biotecnologia, Nutrigenomics Research Group, Universitat Rovira i Virgili, 43007 Tarragona, Spain; Institut d'Investigació Sanitària Pere Virgili, Nutrigenomics Research Group, Universitat Rovira i Virgili, 43007 Tarragona, Spain; Center of Environmental, Food and Toxicological Technology (TecnATox), Nutrigenomics Research Group, University Rovira i Virgili, 43007 Tarragona, Spain*

Lluís Arola − *Departament de Bioquímica i Biotecnologia, Nutrigenomics Research Group, Universitat Rovira i Virgili, 43007 Tarragona, Spain; Institut d'Investigació Sanitària Pere Virgili, Nutrigenomics Research Group, Universitat Rovira i Virgili, 43007 Tarragona, Spain; Center of Environmental, Food and Toxicological Technology (TecnATox), Nutrigenomics Research Group, University Rovira i Virgili, 43007 Tarragona, Spain*

Siu Kwan Sze − *Department of Health Sciences, Faculty of Applied Health Sciences, Brock University, St. Catharines, Ontario L2S 3A1, Canada;* orcid.org/0000-0002-5652-1687

Complete contact information is available at: https://pubs.acs.org/10.1021/acsomega.5c02274

Author Contributions

[¶]M.F.-R. and M.S. contributed equally. Xavier Gallart-Palau and Aida Serra are joint senior authors. Conceptualization: A.S. and X.G-P.; Methodology: M.F-R, M.S., S.S-G., and I.M.; Manuscript draft: A.S. and X.G-P.; Review & editing: A.S., M.S., S.K.S, L.A and X.G-P; Funding acquisition: A.S., X.G-P., M.S. and L.A.; Supervision: A.S., M.S. and X.G-P. All authors have read and approved the submitted version.

Notes

The authors declare no competing financial interest.

ACKNOWLEDGMENTS

Support for this work was provided by the Ministry of Science and Innovation-MCIN, Spain and the National Research Council/Agencia Estatal de Investigación-AEI, Spain (PID2020-114885RB-C21) funded by MCIN/AEI/10.13039/501100011033; The National Institute of Health/Instituto de Salud Carlos III-ISCIII, Spain (PI22/00443 and DTS24/00141; grants cofunded by the European Union); The Spanish Ministry of Science and Innovation with funds from the European Union NextGenerationEU (PRTR-C17.I1); and from the Autonomous Community of Catalonia within the framework of the Biotechnology Plan Applied to Health (EVBRAINTARGET-Y7340-ACPPCCOL007) coordinated by the Institute for Bioengineering of Catalonia (IBEC); The Diputació de Lleida, Spain (PIRS22/03 & PIRS23/02), the Catalan Research Council-AGAUR (2023 LLAV 00056; and 2022 DI 100) and the University of Lleida through (X25022 funded by the call Innovative Projects with Strong Potential for Knowledge or Technology Transfer). The research leading to these results was also supported by the European Commission through its Seventh Framework Programme "BIOmarkers of Robustness of Metabolic Homeostasis for Nutrigenomics-derived Health CLAIMS Made on Food" Project (FP7-KBBE-2009-3 BIOCLAIMS) under grant agreement number 244995. X.G.-P. acknowledges a Miguel Servet program tenure track

https://doi.org/10.1021/acsomega.5c02274
ACS Omega 2025, 10, 23563−23581

contract (CP21/00096) from the ISCIII, awarded on the 2021 call under the Health Strategy Action, cofunded by the European Union (FSE+). A.S. acknowledges a Ramón y Cajal program tenure track contract (RYC2021-030946-I) funded by MCIN/AEI/10.13039/501100011033 and by the "European Union NextGenerationEU/PRTR". M.F.-R.'s postdoctoral contract is funded by PRTR-C17.I1 and EVBRAINTARGET-Y7340-ACPPCCOL007. IRBLLEIDA, X.G.-P., and A.S. are cofunded by the CERCA Program/Generalitat de Catalunya. X.G.-P. is member of the ExoPsyCog Consortium, funded by IKUR-Neurobiosciences—Basque Government.

REFERENCES

(1) Kebekova, A.; Mashirapova, S.; Quadri, G.; Kamran, A.; Yadav, R. Obesity. *Int. Conf.* **2024**, *41* (185), 390−398.
(2) Lafia, A.; Ketounou, T.; Honfoga, J.; Bonou, S.; Zime, A. Dietary Habits, Prevalence of Obesity and Overweight in Developed and Developing Countries. *Res. Soc. Dev.* **2022**, *11*, No. e249111032769.
(3) Lui, D. T. W.; Ako, J.; Dalal, J.; Fong, A.; Fujino, M.; Horton, A.; Krittayaphong, R.; Almahmeed, W.; Matthias, A. T.; Nelson, A. J.; et al. Obesity in the Asia-Pacific Region: Current Perspectives. *J. Asian Pac. Soc. Cardiol.* **2024**, *3*, No. e21.
(4) Kelly, T.; Yang, W.; Chen, C. S.; Reynolds, K.; He, J. Global Burden of Obesity in 2005 and Projections to 2030. *Int. J. Obes.* **2008**, *32* (9), 1431−1437.
(5) Liu, J.; Lai, F.; Hou, Y.; Zheng, R. Leptin Signaling and Leptin Resistance. *Med. Rev.* **2022**, *2* (4), 363−384.
(6) Pena-Leon, V.; Pérez-Lois, R.; Villalón, M.; Prida, E.; Muñoz-Moreno, D.; Fernø, J.; Quiñones, M.; Al-Massadi, O.; Seoane, L. M. Novel Mechanisms Involved in Leptin Sensitization in Obesity. *Biochem. Pharmacol.* **2024**, *223*, 116129.
(7) Ring, L. E.; Zeltser, L. M. Disruption of Hypothalamic Leptin Signaling in Mice Leads to Early-Onset Obesity, but Physiological Adaptations in Mature Animals Stabilize Adiposity Levels. *J. Clin. Invest.* **2010**, *120* (8), 2931−2941.
(8) Bravo-Miana, R. d. C.; Arizaga-Echebarria, J. K.; Otaegui, D. Central Nervous System-Derived Extracellular Vesicles: The Next Generation of Neural Circulating Biomarkers? *Transl. Neurodegener.* **2024**, *13* (1), 32.
(9) van Niel, G.; D'Angelo, G.; Raposo, G. Shedding Light on the Cell Biology of Extracellular Vesicles. *Nat. Rev. Mol. Cell Biol.* **2018**, *19* (4), 213−228.
(10) Théry, C.; Witwer, K. W.; Aikawa, E.; Alcaraz, M. J.; Anderson, J. D.; Andriantsitohaina, R.; Antoniou, A.; Arab, T.; Archer, F.; Atkin-Smith, G. K.; et al. Minimal Information for Studies of Extracellular Vesicles 2018 (MISEV2018): A Position Statement of the International Society for Extracellular Vesicles and Update of the MISEV2014 Guidelines. *J. Extracell. Vesicles* **2018**, *7* (1), 1535750.
(11) Witwer, K. W.; Goberdhan, D. C.; O'Driscoll, L.; Théry, C.; Welsh, J. A.; Blenkiron, C.; Buzas, E. I.; Di Vizio, D.; Erdbrugger, U.; Falcón-Pérez, J. M.; et al. Updating MISEV: Evolving the Minimal Requirements for Studies of Extracellular Vesicles. *J. Extracell. Vesicles* **2021**, *10* (14), No. e12182.
(12) Raposo, G.; Stahl, P. D. Extracellular Vesicles: A New Communication Paradigm? *Nat. Rev. Mol. Cell Biol.* **2019**, *20* (9), 509−510.
(13) Yue, B.; Wang, H.; Cai, X.; Wang, J.; Chai, Z.; Peng, W.; Shu, S.; Fu, C.; Zhong, J. Adipose-Secreted Exosomes and Their Pathophysiologic Effects on Skeletal Muscle. *Int. J. Mol. Sci.* **2022**, *23* (20), 12411.
(14) Yu, Y.; Du, H.; Wei, S.; Feng, L.; Li, J.; Yao, F.; Zhang, M.; Hatch, G. M.; Chen, L. Adipocyte-Derived Exosomal MiR-27a Induces Insulin Resistance in Skeletal Muscle Through Repression of PPARγ. *Theranostics* **2018**, *8* (8), 2171−2188.
(15) Koeck, E. S.; Iordanskaia, T.; Sevilla, S.; Ferrante, S. C.; Hubal, M. J.; Freishtat, R. J.; Nadler, E. P. Adipocyte Exosomes Induce Transforming Growth Factor β Pathway Dysregulation in Hepatocytes: A Novel Paradigm for Obesity-Related Liver Disease. *J. Surg. Res.* **2014**, *192* (2), 268−275.
(16) Yuan, P.; Ding, L.; Chen, H.; Wang, Y.; Li, C.; Zhao, S.; Yang, X.; Ma, Y.; Zhu, J.; Qi, X.; Zhang, Y.; Xia, X.; Zheng, J. C. Neural Stem Cell-Derived Exosomes Regulate Neural Stem Cell Differentiation Through miR-9−Hes1 Axis. *Front. Cell Dev. Biol.* **2021**, *9*, 601600.
(17) Dhanesh, S. B.; Subashini, C.; James, J. Hes1: The Maestro in Neurogenesis. *Cell. Mol. Life Sci.* **2016**, *73* (21), 4019−4042.
(18) Liu, Q.; Tan, Y.; Qu, T.; Zhang, J.; Duan, X.; Xu, H.; Mu, Y.; Ma, H.; Wang, F. Therapeutic Mechanism of Human Neural Stem Cell-Derived Extracellular Vesicles Against Hypoxia−Reperfusion Injury In Vitro. *Life Sci.* **2020**, *254*, 117772.
(19) Lee, E. J.; Choi, Y.; Lee, H. J.; Hwang, D. W.; Lee, D. S. Human Neural Stem Cell-Derived Extracellular Vesicles Protect Against Parkinson's Disease Pathologies. *J. Nanobiotechnol.* **2022**, *20* (1), 198.
(20) Tominaga, N.; Kosaka, N.; Ono, M.; Katsuda, T.; Yoshioka, Y.; Tamura, K.; Lötvall, J.; Nakagama, H.; Ochiya, T. Brain Metastatic Cancer Cells Release MicroRNA-181c−Containing Extracellular Vesicles Capable of Destructing Blood−Brain Barrier. *Nat. Commun.* **2015**, *6*, 6716.
(21) Ridder, K.; et al. Extracellular Vesicle−Mediated Transfer of Genetic Information Between the Hematopoietic System and the Brain in Response to Inflammation. *PLoS Biol.* **2014**, *12* (6), No. e1001874.
(22) Alvarez-Erviti, L.; Seow, Y.; Yin, H.; Betts, C.; Lakhal, S.; Wood, M. J. Delivery of siRNA to the Mouse Brain by Systemic Injection of Targeted Exosomes. *Nat. Biotechnol.* **2011**, *29* (4), 341−345.
(23) Leow, M. K.; Rengaraj, A.; Narasimhan, K.; Verma, S.; Yaligar, J.; Thu, G.; Sun, L.; Goh, H.; Govindharajulu, P.; Sadananthan, S.; et al. Activated brown adipose tissue releases exosomes containing mitochondrial methylene tetrahydrofolate dehydrogenase (NADP dependent) 1-like protein (MTHFD1L). *Biosci. Rep.* **2022**, *42* (5), BSR20212543.
(24) Roy, R.; Lorca, C.; Mulet, M.; Sánchez Milán, J. A.; Baratas, A.; de la Casa, M.; Espinet, C.; Serra, A.; Gallart-Palau, X. Altered Ureido Protein Modification Profiles in Seminal Plasma Extracellular Vesicles of Non-Normozoospermic Men. *Front. Endocrinol.* **2023**, *14*, 1113824.
(25) Gallart-Palau, X.; Guo, X.; Serra, A.; Sze, S. K. Alzheimer's Disease Progression Characterized by Alterations in the Molecular Profiles and Biogenesis of Brain Extracellular Vesicles. *Alzheimers Res. Ther.* **2020**, *12* (1), 54.
(26) Zhang, F.; et al. Brain Extracellular Vesicles in Psychoticism Display Novel Molecular Clues Associated with Age-Related Dementia. *J. Neurol. Sci.* **2023**, *455*, 121393.
(27) Gallart-Palau, X.; et al. Brain-Derived and Circulating Vesicle Profiles Indicate Neurovascular Unit Dysfunction in Early Alzheimer's Disease. *Brain Pathol.* **2019**, *29* (5), 593−605.
(28) Lorca, C.; et al. Next-Generation Proteomics of Brain Extracellular Vesicles in Schizophrenia Provide New Clues on the Altered Molecular Connectome. *Biomedicines* **2024**, *12* (1), 129.
(29) Gallart-Palau, X.; Serra, A.; Sze, S. K. Enrichment of Extracellular Vesicles from Tissues of the Central Nervous System by PROSPR. *Mol. Neurodegener.* **2016**, *11* (1), 41.
(30) Gallart-Palau, X.; Serra, A.; Wong, A. S. W.; Sandin, S.; Lai, M. K. P.; Chen, C. P.; Kon, O. L.; Sze, S. K. Extracellular vesicles are rapidly purified from human plasma by PRotein Organic Solvent PRecipitation (PROSPR). *Sci. Rep.* **2015**, *5*, 14664.
(31) Lorca, C.; Laparra, M.; Céspedes, M. V.; Casaní, L.; Florit, S.; Jové, M.; Mota-Martorell, N.; Vilella, E.; Gallart-Palau, X.; Serra, A. Industrial By-Products as a Novel Circular Source of Biocompatible Extracellular Vesicles. *Adv. Funct. Mater.* **2022**, *32*, 2202700.
(32) Roy, R.; Lorca, C.; Mulet, M.; Sánchez Milán, J. A.; Baratas, A.; de la Casa, M.; Espinet, C.; Serra, A.; Gallart-Palau, X. Altered Ureido Protein Modification Profiles in Seminal Plasma Extracellular Vesicles of Non-Normozoospermic Men. *Front. Endocrinol.* **2023**, *14*, 1113824.

https://doi.org/10.1021/acsomega.5c02274
ACS Omega 2025, 10, 23563−23581

(33) Serra, A.; Gallart-Palau, X.; See-Toh, R. S.; Hemu, X.; Tam, J. P.; Sze, S. K. Commercial Processed Soy-Based Food Product Contains Glycated and Glycoxidated Lunasin Proteoforms. *Sci. Rep.* **2016**, *6*, 26106.
(34) Ishihama, Y.; Oda, Y.; Tabata, T.; Sato, T.; Nagasu, T.; Rappsilber, J.; Mann, M. Exponentially Modified Protein Abundance Index (emPAI) for Estimation of Absolute Protein Amount in Proteomics by the Number of Sequenced Peptides per Protein. *Mol. Cell. Proteomics* **2005**, *4* (9), 1265−1272.
(35) Murari, A.; et al. Dissecting the Concordant and Disparate Roles of NDUFAF3 and NDUFAF4 in Mitochondrial Complex I Biogenesis. *iScience* **2021**, *24* (8), 102869.
(36) Madvig, P.; Abraham, S. Relationship of Malic Enzyme Activity to Fatty Acid Synthesis and the Pathways of Glucose Catabolism in Developing Rat Liver. *J. Nutr.* **1980**, *110* (1), 90−99.
(37) Landrier, J. F.; et al. Reduced Adiponectin Expression after High-Fat Diet Is Associated with Up-Regulation of ALDH1A1 and Retinoic Acid Receptor Signaling in Adipose Tissue. *FASEB J.* **2017**, *31* (1), 203−211.
(38) Lord, C. C.; Thomas, G.; Brown, J. M. Mammalian ABHD Proteins: Lipid Metabolizing Enzymes at the Interface of Cell Signaling and Energy Metabolism. *Biochim. Biophys. Acta* **2013**, *1831* (4), 792−802.
(39) Bravo, E.; et al. Coenzyme Q Metabolism Is Disturbed in High Fat Diet−Induced Nonalcoholic Fatty Liver Disease in Rats. *Int. J. Mol. Sci.* **2012**, *13* (2), 1644−1657.
(40) Hohenstein, B.; et al. Vasodilator-Stimulated Phosphoprotein−Deficient Mice Demonstrate Increased Platelet Activation but Improved Renal Endothelial Preservation in Nephrotoxic Nephritis. *J. Am. Soc. Nephrol.* **2005**, *16* (4), 986−996.
(41) Nassir, F.; et al. Regulation of Mitochondrial Trifunctional Protein Modulates Nonalcoholic Fatty Liver Disease in Mice. *J. Lipid Res.* **2018**, *59* (6), 967−973.
(42) Tacke, F.; Horn, P.; Wai-Sun Wong, V.; Ratziu, V.; Bugianesi, E.; Francque, S.; Zelber-Sagi, S.; Valenti, L.; Roden, M.; Schick, F.; et al. EASL−EASD−EASO Clinical Practice Guidelines on the Management of Metabolic Dysfunction−Associated Steatotic Liver Disease (MASLD). *J. Hepatol.* **2024**, *81*, 492−542.
(43) Shi, L.; et al. Comparison of Protective Effects of Hesperetin and Pectolinarigenin on High-Fat Diet−Induced Hyperlipidemia and Hepatic Steatosis in Golden Syrian Hamsters. *Exp. Anim.* **2023**, *72* (1), 123−131.
(44) Suárez-García, S.; Caimari, A.; del Bas, J. M.; Suárez, M.; Arola, L. Serum Lysophospholipid Levels Are Altered in Dyslipidemic Hamsters. *Sci. Rep.* **2017**, *7* (1), 10431.
(45) Ha, S. Y.; et al. Expression of Prothymosin α Predicts Early Recurrence and Poor Prognosis of Hepatocellular Carcinoma. *Hepatobiliary Pancreatic Dis. Int.* **2015**, *14* (2), 171−177.
(46) Liu, J.; Zhao, K.; Wu, S.; Li, C.; You, C.; Wang, J.; Shu, K.; Lei, T. The Dual Role of PDCD10 in Cancers: A Promising Therapeutic Target. *Cancers* **2022**, *14* (23), 5986.
(47) Wesoly, J.; et al. Structural, Topological, and Functional Characterization of Transmembrane Proteins (TMEM213, 207, 116, 72, and 30B) Provides a Potential Link to ccRCC Etiology. *Am. J. Cancer Res.* **2023**, *13* (5), 1863−1883.
(48) Chiappetta, G.; et al. Detection of high mobility group I HMGI(Y) protein in the diagnosis of thyroid tumors: HMGI(Y) expression represents a potential diagnostic indicator of carcinoma. *Cancer Res.* **1998**, *58* (18), 4193−4198.
(49) Khoury, W. E.; Nasr, Z. Deregulation of Ribosomal Proteins in Human Cancers. *Biosci. Rep.* **2021**, *41* (12), BSR20211577.
(50) Enomoto, H.; et al. Hepatoma-Derived Growth Factor: Its Possible Involvement in the Progression of Hepatocellular Carcinoma. *Int. J. Mol. Sci.* **2015**, *16* (6), 14086−14097.
(51) Skawran, B.; et al. Gene Expression Profiling in Hepatocellular Carcinoma: Upregulation of Genes in Amplified Chromosome Regions. *Mod. Pathol.* **2008**, *21* (5), 505−516.
(52) Raturi, A.; et al. TMX1 Determines Cancer Cell Metabolism as a Thiol-Based Modulator of ER−Mitochondria Ca^{2+} Flux. *J. Cell Biol.* **2016**, *214* (4), 433−444.
(53) Comuzzie, A. G.; et al. Novel Genetic Loci Identified for the Pathophysiology of Childhood Obesity in the Hispanic Population. *PLoS One* **2012**, *7* (12), No. e51954.
(54) Oh, J.; et al. METTL3-Mediated Downregulation of Splicing Factor SRSF11 Is Associated with Carcinogenesis and Poor Survival of Cancer Patients. *Eur. Rev. Med. Pharmacol. Sci.* **2023**, *27* (6), 2561−2570.
(55) Caner, A.; Asik, E.; Ozpolat, B. SRC Signaling in Cancer and Tumor Microenvironment. *Adv. Exp. Med. Biol.* **2021**, *1270*, 57−71.
(56) Doyle, K. M.; et al. Unfolded Proteins and Endoplasmic Reticulum Stress in Neurodegenerative Disorders. *J. Cell. Mol. Med.* **2011**, *15* (10), 2025−2039.
(57) Perot, B. P.; Menager, M. M. Tetraspanin 7 and Its Closest Paralog Tetraspanin 6: Membrane Organizers with Key Functions in Brain Development, Viral Infection, Innate Immunity, Diabetes, and Cancer. *Med. Microbiol. Immunol.* **2020**, *209* (4), 427−436.
(58) Chiu, D. K.; et al. Hepatocellular Carcinoma Cells Up-Regulate PVRL1, Stabilizing PVR and Inhibiting the Cytotoxic T-Cell Response via TIGIT to Mediate Tumor Resistance to PD1 Inhibitors in Mice. *Gastroenterology* **2020**, *159* (2), 609−623.
(59) Ahlers, K. E.; Chakravarti, B.; Fisher, R. A. RGS6 as a Novel Therapeutic Target in CNS Diseases and Cancer. *AAPS J.* **2016**, *18* (3), 560−572.
(60) Zhi, X.; et al. E3 Ubiquitin Ligase RNF126 Promotes Cancer Cell Proliferation by Targeting the Tumor Suppressor p21 for Ubiquitin-Mediated Degradation. *Cancer Res.* **2013**, *73* (1), 385−394.
(61) Aasen, T.; et al. Connexins in Cancer: Bridging the Gap to the Clinic. *Oncogene* **2019**, *38* (23), 4429−4451.
(62) Gelis, L.; et al. Functional Expression of Olfactory Receptors in Human Primary Melanoma and Melanoma Metastasis. *Exp. Dermatol.* **2017**, *26* (7), 569−576.
(63) Yuan, Y.; Nie, H. Protein Arginine Methyltransferase 5: A Potential Cancer Therapeutic Target. *Cell. Oncol.* **2021**, *44* (1), 33−44.
(64) Si, L.; Liu, L.; Yang, R.; Li, W.; Xu, X. High Expression of TARS Is Associated with Poor Prognosis of Endometrial Cancer. *Aging* **2023**, *15* (5), 1524−1542.
(65) Li, Y.; et al. Cancer Driver Candidate Genes AVL9, DENND5A and NUPL1 Contribute to MDCK Cystogenesis. *Oncoscience* **2014**, *1* (12), 854−865.
(66) Jang, S.; et al. Differential Role for Phosphorylation in Alternative Polyadenylation Function versus Nuclear Import of SR-Like Protein CPSF6. *Nucleic Acids Res.* **2019**, *47* (9), 4663−4683.
(67) Hwang, J. W.; et al. Protein Arginine Methyltransferases: Promising Targets for Cancer Therapy. *Exp. Mol. Med.* **2021**, *53* (5), 788−808.
(68) Kristensen, L. S.; et al. Circular RNAs in Cancer: Opportunities and Challenges in the Field. *Oncogene* **2018**, *37* (5), 555−565.
(69) Liu, P.; Cheng, H.; Roberts, T. M.; Zhao, J. J. Targeting the Phosphoinositide 3-Kinase Pathway in Cancer. *Nat. Rev. Drug Discovery* **2009**, *8* (8), 627−644.
(70) Peppino, G.; Ruiu, R.; Arigoni, M.; Riccardo, F.; Iacoviello, A.; Barutello, G.; Quaglino, E. Teneurins: Role in Cancer and Potential Role as Diagnostic Biomarkers and Targets for Therapy. *Int. J. Mol. Sci.* **2021**, *22* (5), 2321.
(71) Voncken, J. W.; et al. Bcr/Abl Associated Leukemogenesis in bcr Null Mutant Mice. *Oncogene* **1998**, *16* (15), 2029−2032.
(72) Cheng, S.; et al. Transforming Acidic Coiled-Coil−Containing Protein 2 (TACC2) in Human Breast Cancer: Expression Pattern and Clinical/Prognostic Relevance. *Cancer Genomics Proteomics* **2010**, *7* (2), 67−73.
(73) Du, Y.; Grandis, J. R. Receptor-Type Protein Tyrosine Phosphatases in Cancer. Chin. *J. Cancer* **2015**, *34* (2), 61−69.
(74) Ghiselli, G. SMC3 Knockdown Triggers Genomic Instability and p53-Dependent Apoptosis in Human and Zebrafish Cells. *Mol. Cancer* **2006**, *5*, 52.

https://doi.org/10.1021/acsomega.5c02274
ACS Omega 2025, 10, 23563−23581

(75) Molee, P.; et al. Up-Regulation of AKAP13 and MAGT1 on Cytoplasmic Membrane in Progressive Hepatocellular Carcinoma: A Novel Target for Prognosis. *Int. J. Clin. Exp. Pathol.* **2015**, *8* (9), 9796−9811.
(76) Cesi, G.; Walbrecq, G.; Margue, C.; Kreis, S. Transferring Intercellular Signals and Traits between Cancer Cells: Extracellular Vesicles as "Homing Pigeons". *Cell Commun. Signaling* **2016**, *14* (1), 13.
(77) Gruosso, T.; et al. Chronic Oxidative Stress Promotes H2AX Protein Degradation and Enhances Chemosensitivity in Breast Cancer Patients. *EMBO Mol. Med.* **2016**, *8* (5), 527−549.
(78) Miranda, M. A.; St Pierre, C. L.; Macias-Velasco, J. F.; Nguyen, H. A.; Schmidt, H.; Agnello, L. T.; Wayhart, J. P.; Lawson, H. A. Dietary Iron Interacts with Genetic Background to Influence Glucose Homeostasis. *Nutr. Metab.* **2019**, *16*, 13.
(79) Wang, X.; Song, H.; Liang, J.; Jia, Y.; Zhang, Y. Abnormal expression of HADH, an enzyme of fatty acid oxidation, affects tumor development and prognosis (Review). *Mol. Med. Rep.* **2022**, *26* (6), 355.
(80) Xu, J.; et al. RhoGAPs Attenuate Cell Proliferation by Direct Interaction with p53 Tetramerization Domain. *Cell Rep.* **2013**, *3* (5), 1526−1538.
(81) Peng, D. F.; et al. Silencing of Glutathione Peroxidase 3 through DNA Hypermethylation Is Associated with Lymph Node Metastasis in Gastric Carcinomas. *PLoS One* **2012**, *7* (10), No. e46214.
(82) Liu, K.; Wang, G.; Ding, H.; Chen, Y.; Yu, G.; Wang, J. Downregulation of Metastasis Suppressor 1 (MTSS1) Is Associated with Nodal Metastasis and Poor Outcome in Chinese Patients with Gastric Cancer. *BMC Cancer* **2010**, *10*, 428.
(83) Liu, X.; Zhang, W.; Wang, H.; Zhu, L.; Xu, K. Decreased Expression of ACADSB Predicts Poor Prognosis in Clear Cell Renal Cell Carcinoma. *Front. Oncol.* **2022**, *11*, 762629.
(84) Li, L.; et al. The Human Cadherin 11 Is a Pro-Apoptotic Tumor Suppressor Modulating Cell Stemness through Wnt/β-Catenin Signaling and Silenced in Common Carcinomas. *Oncogene* **2012**, *31* (34), 3901−3912.
(85) Chen, J.; et al. Identification of Key Candidate Genes Involved in Melanoma Metastasis. *Mol. Med. Rep.* **2019**, *20* (2), 903−914.
(86) Tan, H.; et al. The Role of 14−3-3 in the Progression of Vascular Inflammation Induced by Lipopolysaccharide. *Int. Immunopharmacol.* **2023**, *119*, 110220.
(87) Leidi, M.; et al. EDF-1 Contributes to the Regulation of Nitric Oxide Release in VEGF-Treated Human Endothelial Cells. *Eur. J. Cell Biol.* **2010**, *89* (9), 654−660.
(88) Siegel-Axel, D. I.; et al. Fetuin-A Influences Vascular Cell Growth and Production of Proinflammatory and Angiogenic Proteins by Human Perivascular Fat Cells. *Diabetologia* **2014**, *57* (5), 1057−1066.
(89) Edamatsu, M.; et al. Hapln4/Bral2 Is a Selective Regulator for Formation and Transmission of GABAergic Synapses between Purkinje and Deep Cerebellar Nuclei Neurons. *J. Neurochem.* **2018**, *147* (6), 748−763.
(90) Gumina, R. J.; et al. Na^+/H^+ Exchange Inhibition Prevents Endothelial Dysfunction after I/R Injury. *Am. J. Physiol. Heart Circ. Physiol.* **2001**, *281* (3), H1260−H1266.
(91) Kardys, I.; et al. Fibrinogen Gene Haplotypes in Relation to Risk of Coronary Events and Atherosclerosis: The Rotterdam Study. *Thromb. Haemostasis* **2007**, *97* (2), 288−295.
(92) Park, S. G.; Schimmel, P.; Kim, S. Aminoacyl tRNA Synthetases and Their Connections to Disease. *Proc. Natl. Acad. Sci. U.S.A.* **2008**, *105* (32), 11043−11049.
(93) Zheng, Y.; et al. Angiomotin-Like Protein 1 Controls Endothelial Polarity and Junction Stability during Sprouting Angiogenesis. *Circ. Res.* **2009**, *105* (3), 260−270.
(94) Li, Q.; et al. A Homozygous Stop-Gain Variant in ARHGAP42 Is Associated with Childhood Interstitial Lung Disease, Systemic Hypertension, and Immunological Findings. *PLoS Genet.* **2021**, *17* (7), No. e1009639.
(95) Han, Y.; et al. Formin-Like 1 (FMNL1) Is Regulated by N-Terminal Myristoylation and Induces Polarized Membrane Blebbing. *J. Biol. Chem.* **2009**, *284* (48), 33409−33417.
(96) Chen, Y. F.; et al. Cisd2Mediates Mitochondrial Integrity and Life Span in Mammals. *Autophagy* **2009**, *5* (7), 1043−1045.
(97) Møller, L. L. V.; Nielsen, I. L.; Knudsen, J. R.; Andersen, N. R.; Jensen, T. E.; Sylow, L.; Richter, E. A. The p21-Activated Kinase 2 (PAK2), but Not PAK1, Regulates Contraction-Stimulated Skeletal Muscle Glucose Transport. *Physiol. Rep.* **2020**, *8* (12), No. e14460.
(98) Palmieri, F. The Mitochondrial Transporter Family SLC25: Identification, Properties and Physiopathology. *Mol. Aspects Med.* **2013**, *34* (2−3), 465−484.
(99) Jonckheere, A. I.; et al. Mitochondrial ATP Synthase: Architecture, Function and Pathology. *J. Inherited Metab. Dis.* **2012**, *35* (2), 211−225.
(100) Way, K. J.; Chou, E.; King, G. L. Identification of PKC-Isoform-Specific Biological Actions Using Pharmacological Approaches. *Trends Pharmacol. Sci.* **2000**, *21* (5), 181−187.
(101) Lee, H. T.; Emala, C. W. Protective Effects of Renal Ischemic Preconditioning and Adenosine Pretreatment: Role of A_1 and A_3 Receptors. *Am. J. Physiol. Renal Physiol.* **2000**, *278* (3), F380−F387.
(102) Liang, F.; Wang, B.; Geng, J.; You, G.; Fa, J.; Zhang, M.; Sun, H.; Chen, H.; Fu, Q.; Zhang, X.; et al. SORBS2 Is a Genetic Factor Contributing to Cardiac Malformation of 4q Deletion Syndrome Patients. *Elife* **2021**, *10*, No. e67481.
(103) Elghazi, L.; Gould, A. P.; Weiss, A. J.; Barker, D. J.; Callaghan, J.; Opland, D.; Myers, M.; Cras-Méneur, C.; Bernal-Mizrachi, E. Importance of β-Catenin in Glucose and Energy Homeostasis. *Sci. Rep.* **2012**, *2*, 693.
(104) Celikbilek, A.; et al. S100B as a Glial Cell Marker in Diabetic Peripheral Neuropathy. *Neurosci. Lett.* **2014**, *558*, 53−57.
(105) Watanabe, J.; et al. Role of IGFBP7 in Diabetic Nephropathy: TGF-β1 Induces IGFBP7 via Smad2/4 in Human Renal Proximal Tubular Epithelial Cells. *PLoS One* **2016**, *11* (3), No. e0150897.
(106) Ihara, Y.; et al. Increased Expression of Protein C-Mannosylation in the Aortic Vessels of Diabetic Zucker Rats. *Glycobiology* **2005**, *15* (4), 383−392.
(107) Bueno, D.; et al. NECAB2 Is an Endosomal Protein Important for Striatal Function. *Free Radical Biol. Med.* **2023**, *208*, 643−656.
(108) Udagawa, H.; Funahashi, N.; Nishimura, W.; Uebanso, T.; Kawaguchi, M.; Asahi, R.; Nakajima, S.; Nammo, T.; Hiramoto, M.; Yasuda, K. Glucocorticoid Receptor−NECAB1 Axis Can Negatively Regulate Insulin Secretion in Pancreatic β-Cells. *Sci. Rep.* **2023**, *13* (1), 17958.
(109) Kwok, Y. C.; et al. Kinetic Properties of the Insulin Receptor Tyrosine Protein Kinase: Activation through an Insulin-Stimulated Autophosphorylation. *Arch. Biochem. Biophys.* **1986**, *244* (1), 102−113.
(110) Wang, Y.; et al. BRSK2 Is Regulated by ER Stress in Protein Level and Involved in ER Stress−Induced Apoptosis. *Biochem. Biophys. Res. Commun.* **2012**, *423* (4), 813−818.
(111) Wittig, R.; Coy, J. F. The Role of Glucose Metabolism and Glucose-Associated Signaling in Cancer. *Perspect. Med. Chem.* **2008**, *1*, 64−82.
(112) Bobrich, M.; et al. PTPIP51 Interaction with PTP1B and 14−3-3β in Adipose Tissue of Insulin-Resistant Mice. *Int. J. Obes.* **2011**, *35* (11), 1385−1394.
(113) Tang, W. J. Targeting Insulin-Degrading Enzyme to Treat Type 2 Diabetes Mellitus. *Trends Endocrinol. Metab.* **2016**, *27* (1), 24−34.
(114) Minarovic, I.; et al. Effect of the High-Fat Diet on the Calcium Channels in Rat Myocardium. *Ann. N.Y. Acad. Sci.* **1997**, *827*, 550−555.
(115) Xie, J.; et al. Negative Regulation of Grb10 Interacting GYF Protein 2 on IGF-1 Receptor Signaling Causes Diabetic Mice Cognitive Impairment. *PLoS One* **2014**, *9* (9), No. e108559.
(116) Holmkvist, J.; et al. Polymorphisms in the Gene Encoding the Voltage-Dependent Ca^{2+} Channel Ca(V)2.3 (CACNA1E) Are

https://doi.org/10.1021/acsomega.5c02274
ACS Omega 2025, 10, 23563−23581

Associated with Type 2 Diabetes and Impaired Insulin Secretion. *Diabetologia* **2007**, *50* (12), 2467−2475.
(117) Santulli, G.; et al. Calcium Release Channel RyR2 Regulates Insulin Release and Glucose Homeostasis. *J. Clin. Invest.* **2015**, *125* (5), 1968−1978.
(118) Yun, H. S.; et al. Knockdown of Hepatoma-Derived Growth Factor−Related Protein-3 Induces Apoptosis via ROS-Dependent and p53-Independent NF-κB Activation in H1299 Cells. *Biochem. Biophys. Res. Commun.* **2014**, *449* (4), 471−476.
(119) Yu, C. H.; et al. Key Genes and Regulatory Networks for Diabetic Retinopathy Based on Hypoxia-Related Genes: A Bioinformatics Analysis. *Int. J. Ophthalmol.* **2024**, *17* (8), 1411−1417.
(120) Kimple, M. E.; Neuman, J. C.; Linnemann, A. K.; Casey, P. J. Inhibitory G Proteins and Their Receptors: Emerging Therapeutic Targets for Obesity and Diabetes. *Exp. Mol. Med.* **2014**, *46* (6), No. e102.
(121) Aljaibeji, H.; Mukhopadhyay, D.; Mohammed, A. K.; Dhaiban, S.; Hachim, M. Y.; Elemam, N. M.; Sulaiman, N.; Salehi, A.; Taneera, J. Reduced Expression of PLCXD3 Associates with Disruption of Glucose Sensing and Insulin Signaling in Pancreatic β-Cells. *Front. Endocrinol. (Lausanne)* **2019**, *10*, 735.
(122) Varadaiah, Y. G. C.; et al. Purine Metabolites Can Indicate Diabetes Progression. *Arch. Physiol. Biochem.* **2022**, *128* (1), 87−91.
(123) Chu, C. H.; Cheng, D. Expression, Purification, and Characterization of Human 3-Methylcrotonyl-CoA Carboxylase (MCCC). *Protein Expression Purif.* **2007**, *53* (2), 421−427.
(124) Tang, H.; et al. Genes−Environment Interactions in Obesity- and Diabetes-Associated Pancreatic Cancer: A GWAS Data Analysis. *Cancer Epidemiol., Biomarkers Prev.* **2014**, *23* (1), 98−106.
(125) Norman, M.; et al. The Increasing Diversity of Functions Attributed to the SAFB Family of RNA/DNA-Binding Proteins. *Biochem. J.* **2016**, *473* (23), 4271−4288.
(126) Velotti, F.; Barchetta, I.; Cimini, F. A.; Cavallo, M. G. Granzyme B in Inflammatory Diseases: Apoptosis, Inflammation, ECM Remodeling, EMT, and Fibrosis. *Front. Immunol.* **2020**, *11*, 587581.
(127) Sahara, S.; et al. Acinus Is a Caspase-3−Activated Protein Required for Apoptotic Chromatin Condensation. *Nature* **1999**, *401* (6749), 168−173.
(128) Rhee, S. G.; Woo, H. A.; Kil, I. S.; Bae, S. H. Peroxiredoxin Functions as a Peroxidase and as a Regulator/Sensor of Local Peroxides. *J. Biol. Chem.* **2012**, *287* (7), 4403−4410.
(129) Oh, C. K.; et al. FAM213A Is Linked to Prognostic Significance in Acute Myeloid Leukemia through Regulation of Oxidative Stress and Myelopoiesis. *Hematol. Oncol.* **2020**, *38* (3), 381−389.
(130) Leopold, J. A.; Loscalzo, J. Oxidative Risk for Atherothrombotic Cardiovascular Disease. *Free Radical Biol. Med.* **2009**, *47* (12), 1673−1706.
(131) Kajimura, S.; et al. Regulation of the Brown and White Fat Gene Programs through a PRDM16/CtBP Transcriptional Complex. *Genes Dev.* **2008**, *22* (10), 1397−1409.
(132) Xia, Y.; et al. Pathogenic Mutation of UBQLN2 Impairs Its Interaction with UBXD8 and Disrupts ER-Associated Protein Degradation. *J. Neurochem.* **2014**, *129* (1), 99−106.
(133) Russell, J. C.; Proctor, S. D. Small Animal Models of Cardiovascular Disease: Tools for the Study of Metabolic Syndrome, Dyslipidemia, and Atherosclerosis. *Cardiovasc. Pathol.* **2006**, *15* (6), 318−330.
(134) Calderon-Perez, L.; et al. Serum Lysophospholipidome of Dietary Origin as a Susceptibility/Risk Biomarker of Human Hypercholesterolemia: A Cross-Sectional Study. *Clin. Nutr.* **2022**, *41* (2), 489−499.
(135) Tran, L. T.; et al. Hypothalamic Control of Energy Expenditure and Thermogenesis. *Exp. Mol. Med.* **2022**, *54* (4), 358−369.
(136) Le Thuc, O.; Stobbe, K.; Cansell, C.; Nahon, J. L.; Blondeau, N.; Rovère, C. Hypothalamic Inflammation and Energy Balance Disruptions: Spotlight on Chemokines. *Front. Endocrinol.* **2017**, *8*, 197.
(137) Kim, C. Y.; Ahn, J. H.; Han, D. H.; NamKoong, C.; Choi, H. J. Proteome Analysis of the Hypothalamic Arcuate Nucleus in Chronic High-Fat Diet−Induced Obesity. *Biomed. Res. Int.* **2021**, *2021*, 3501770.
(138) McLean, F. H.; Campbell, F. M.; Langston, R. F.; Sergi, D.; Resch, C.; Grant, C.; Morris, A. C.; Mayer, C. D.; Williams, L. M. A High-Fat Diet Induces Rapid Changes in the Mouse Hypothalamic Proteome. *Nutr. Metab.* **2019**, *16*, 26.
(139) Winkelkotte, A. M.; Al-Shami, K.; Chaves-Filho, A. B.; Vogel, F. C.; Schulze, A. Interactions of Fatty Acid and Cholesterol Metabolism with Cellular Stress Response Pathways in Cancer. *Cold Spring Harbor Perspect. Med.* **2024**, *15*, a041548.
(140) Lopes, R.; Santana, M. S.; Costa, P. I. D.; Gaspar, A. M. M.; Cruz, C. R. D.; Fulindi, R. Central Cellular Signaling Pathways Involved in the Regulation of Lipid Metabolism in the Liver: A Review. *Acta Sci. Biol. Sci.* **2020**, *42*, No. e51151.
(141) Povero, D.; et al. Circulating Extracellular Vesicles with Specific Proteome and Liver microRNAs Are Potential Biomarkers for Liver Injury in Experimental Fatty Liver Disease. *PLoS One* **2014**, *9* (12), No. e113651.
(142) Wang, Z.; et al. Extracellular Vesicles in Fatty Liver Promote a Metastatic Tumor Microenvironment. *Cell Metab.* **2023**, *35* (7), 1209−1226.
(143) Szabo, G.; Momen-Heravi, F. Extracellular Vesicles in Liver Disease and Their Potential as Biomarkers and Therapeutic Targets. *Nat. Rev. Gastroenterol. Hepatol.* **2017**, *14* (8), 455−466.
(144) Wirtenberger, M.; et al. Association of Genetic Variants in the Rho Guanine Nucleotide Exchange Factor AKAP13 with Familial Breast Cancer. *Carcinogenesis* **2006**, *27* (3), 593−598.
(145) Paredes, M. R.; Schütz, S.; Boldo, L. S.; Lonsdorf, A.; Lyko, F. 237 Cancer-associated fibroblasts with distinct origins and functions establish a pro-tumorigenic environment in squamous cell carcinoma. *J. Invest. Dermatol.* **2023**, *143*, S41.
(146) Mehner, C.; et al. Tumor Cell−Derived MMP3 Orchestrates Rac1b and Tissue Alterations That Promote Pancreatic Adenocarcinoma. *Mol. Cancer Res.* **2014**, *12* (10), 1430−1439.
(147) Dabrowska, A.; Tarach, J. S.; Wojtysiak-Duma, B.; Duma, D. Fetuin-A (AHSG) and Its Usefulness in Clinical Practice: A Review. *Biomed. Pap. Med. Fac. Univ. Palacky, Olomouc, Czechoslovakia* **2015**, *159*, 352−359.
(148) Haj-Mirzaian, A.; Ramezanzadeh, K.; Shariatzadeh, S.; Tajik, M.; Khalafi, F.; Tafazolimoghadam, A.; Radmard, M.; Rahbar, A.; Pirri, F.; Kazemi, K.; et al. Role of hypothalamic-pituitary adrenal-axis, toll-like receptors, and macrophage polarization in pre-atherosclerotic changes induced by social isolation stress in mice. *Sci. Rep.* **2021**, *11* (1), 19091.
(149) Corraliza-Gomez, M.; Bermejo, T.; Lilue, J.; Rodriguez-Iglesias, N.; Valero, J.; Cozar-Castellano, I.; Arranz, E.; Sanchez, D.; Ganfornina, M. D. Insulin-degrading enzyme (IDE) as a modulator of microglial phenotypes in the context of Alzheimer's disease and brain aging. *J. Neuroinflammation* **2023**, *20* (1), 233.
(150) Stepien, M.; Rosniak-Bak, K.; Paradowski, M.; Misztal, M.; Kujawski, K.; Banach, M.; Rysz, J. Waist circumference, ghrelin and selected adipose tissue-derived adipokines as predictors of insulin resistance in obese patients: Preliminary results. *Med. Sci. Monit.* **2011**, *17* (11), Pr13−Pr18.
(151) Katsareli, E. A.; Dedoussis, G. Biomarkers in the Field of Obesity and Its Related Comorbidities. *Expert Opin. Ther. Targets* **2014**, *18* (4), 385−401.
(152) Kuneš, J.; Hojná, S.; Mráziková, L.; Montezano, A.; Touyz, R.; Maletínská, L. Obesity, Cardiovascular and Neurodegenerative Diseases: Potential Common Mechanisms. *Physiol. Res.* **2023**, *72* (Suppl 2), S73−S90.
(153) Milbank, E.; et al. Extracellular Vesicles: Pharmacological Modulators of Peripheral and Central Signals Governing Obesity. *Pharmacol. Ther.* **2016**, *157*, 65−83.

https://doi.org/10.1021/acsomega.5c02274
ACS Omega 2025, 10, 23563−23581

(154) Zhai, R.; et al. Genetic and Phenotypic Links between Obesity and Extracellular Vesicles. *Hum. Mol. Genet.* **2022**, *31* (21), 3643−3651.

https://doi.org/10.1021/acsomega.5c02274
ACS Omega 2025, 10, 23563−23581